JUHAN SAARING

Ultrafast Relaxation Processes
in Ternary Hexafluorides Studied
under Synchrotron Radiation Excitation

TARTU ÜLIKOOL
UNIVERSITAS TARTUENSIS
1632

DISSERTATIONES PHYSICAE UNIVERSITATIS TARTUENSIS

130

JUHAN SAARING

Ultrafast Relaxation Processes
in Ternary Hexafluorides Studied
under Synchrotron Radiation Excitation

This study was carried out at the Institute of Physics, University of Tartu, Estonia.

The dissertation was admitted on 08.06.2022, in partial fulfilment of the requirements for the degree of Doctor of Philosophy in physics and was allowed for defence by the Scientific Council of the Institute of Physics, University of Tartu.

Supervisor: Prof. Marco Kirm, PhD
                Institute Physics, University of Tartu, Estonia

Opponent: Asst. Prof. Mauro Fasoli
                Department of Materials Science
                University of Milano Bicocca

Defence: 30.08.2022 at University of Tartu, Tartu, Estonia

European Union
European Regional
Development Fund

Investing
in your future

University of Tartu Press
www.tyk.ee

CONTENTS

LIST OF PUBLICATIONS INCLUDED IN THE THESIS

I   **J. Saaring**, E. Feldbach, V. Nagirnyi, S. Omelkov, A. Vanetsev, M. Kirm, Ultrafast radiative relaxation processes in multication cross-luminescence materials, IEEE Transactions on Nuclear Science **67** (2020) 1009–1013, doi:10.1109/TNS.2020.2974071.

II   **J. Saaring**, A. Vanetsev, K. Chernenko, E. Feldbach, I. Kudryavtseva, H. Mändar, R. Pärna, V. Nagirnyi, S. Omelkov, I. Romet, O. Rebane, M. Kirm, Relaxation of electronic excitations in K_2GeF_6 studied by means of time-resolved luminescence spectroscopy under VUV and pulsed electron beam excitation, Journal of Alloys and Compounds **883** (2021) 160916, doi: 10.1016/j.jallcom.2021.160916.

III **J. Saaring**, A. Vanetsev, K. Chernenko, E. Feldbach, I. Kudryavtseva, H. Mändar, S. Pikker, R. Pärna, V. Nagirnyi, S. Omelkov, I. Romet, O. Rebane, M. Kirm, Time-resolved luminescence spectroscopy of ultrafast emissions in $BaGeF_6$, Journal of Luminescence **244** (2022) 118729, doi: 10.1016/j.jlumin.2022.118729.

IV   S.I. Omelkov, K. Chernenko, J.C. Ekström, A. Jurgilaitis, A. Khadiev, A. Kivimäki, A. Kotlov, D. Kroon, J. Larsson, V. Nagirnyi, D.V. Novikov, V.-T. Pham, R. Pärna, I. Romet, **J. Saaring**, I. Schostak, E. Tiirinen, A. Tõnisoo, M. Kirm, Recent advances in time-resolved luminescence spectroscopy at MAX IV and PETRA III storage rings, Journal of Physics: Conference Series. Proceedings of the 14th International Conference on Synchrotron Radiation Instrumentation (2022) in press.

AUTHOR'S CONTRIBUTION

The author was responsible for preparation and performing luminescence investigation under synchrotron radiation and electron-beam excitation, followed by data analysis of the experimental results. The author was responsible for writing the manuscripts in cooperation with the co-authors and for the publishing process. The author also contributed to the development of a new luminescence setup used at FemtoMAX and its implementation.

OTHER PUBLICATIONS OF THE DISSERTANT

1. R. M. Turtos, S. Gundacker, S. Omelkov, B. Mahler, A. H. Khan, **J. Saaring**, Z. Meng, A. Vasil'ev, C. Dujardin, M. Kirm, I. Moreels, E. Auffray, P. Lecoq, On the use of CdSe scintillating nanoplatelets as time taggers for high-energy gamma detection, npj 2D Materials and Applications **3** (2019) 37, doi: 10.1038/s41699-019-0120-8.

LIST OF ABBREVIATIONS

CL	cross-luminescence
CMS	Compact Muon Solenoid
CTR	coincidence time resolution
DOS	density of states
FD	focal distance
FWHM	full width at half maximum
IBL	intraband luminescence
iCCD	intensified charge coupled device
ILY	intrinsic light yield
IRF	instrumental response function
LINAC	linear accelerator
LNT	liquid nitrogen temperature
LSO	Lu_2SiO_5
MCP-PMT	microchannel plate photomultiplier tube
PDE	photon detection efficiency
PET	positron-emission tomography
PL	photoluminescence
PLES	photoluminescence endstation
SEM	scanning electron microscopy
SiPM	silicon-photomultiplier
SNR	signal-to-noise ratio
SPAD	single photon avalanche diode
SR	synchrotron radiation
STE	self-trapped exciton
STW	short-time window
TOF	time-of-flight
TSL	thermally stimulated luminescence
UV	ultraviolet
VUV	vacuum ultraviolet
XRD	x-ray diffraction analysis

1. INTRODUCTION

Scintillator materials have a wide range of application from simple ionizing radiation detection to sophisticated medical and scientific applications. Research and development of novel scintillator materials aims to meet the demands of the applying industries [1]. One of the branches of scintillator research is focused on developing materials to be used in various fast timing applications. Current work will give an overview of the current challenges in this field and possible solutions.

Scintillator materials with fast timing performance are applied for example in high energy physics experiments to prevent pile-up events at high signal levels and in homeland security to allow for fast screening and precise detection of illicit substances. Great effort is also put into the development of scintillators to increase signal-to-noise ratio (SNR) in time-of-flight positron emission tomography (TOF-PET), a valuable medical diagnostic imaging application used to locate and plan the treatment of cancerous tumours. In order to significantly increase the level of detail of TOF-PET studies and at the same time decrease study time and patient dose, an ambitious goal of 10 ps time resolution has been set [2]. Relaxation processes leading to fast luminescence in current established scintillator materials based on rare earth dopant ions (*e.g.,* Ce^{3+} and Pr^{3+}) are intrinsically too slow to achieve this goal and therefore a fundamentally different approach has to be considered.

In this work, the advantages and disadvantages of intrinsic luminescence processes, which could lead to significantly improved time resolution are discussed. Band structure engineering approach is used to demonstrate overcoming some of the disadvantages in using intrinsic emissions. The properties of cross-luminescence (CL) and intraband luminescence (IBL) in ternary hexafluorides studied under synchrotron radiation excitation are brought as an example.

2. OVERVIEW OF THE CURRENT SITUATION IN THE FIELD OF SCINTILLATOR RESEARCH

General requirements for scintillator materials to be used in fast timing applications

The time resolution of a detector system is defined by the precision of the time stamp attributed to the detection of a particle [2]. The chain of events starts with an interaction between high-energy radiation and the scintillator material and ends with the digitalisation of the electric impulse from the photodetector readout. Each interaction including and between these events influences the time resolution of the detector system. This work is focused on the properties of the scintillator material and luminescence light emerging from its initial interaction with high energy radiation.

Generally desired properties that define the efficiency of scintillators include high density, radiation hardness, high light yield and good transmittance. Additionally, a number of practical technological properties such as chemical stability, malleability and production cost influence the applicability of the material. Scintillator materials to be applied in fast timing applications must feature additional characteristics to meet the high demands of target applications. Coincidence time resolution (CTR) is used to describe the time resolution of a detector system in time-of-flight (TOF) applications and is expressed as FWHM of the distribution of time difference measurements [3]. For example, in case of TOF-PET, CTR expresses the detector systems' ability to localize the positron annihilation event along the line-of-response, *i.e.,* lower CTR expresses the ability to localize the source of positron radiation more accurately, which in turn leads to increased SNR [2]. CTR of a detector system is a function of scintillator emission rise time τ_r and decay time τ_d and intrinsic light yield (ILY) [4].

$$\text{CTR} \propto \sqrt{\frac{\tau_r \tau_d}{\text{ILY}}} \qquad \text{(Eq. 1)}$$

High ILY is almost always desired in scintillator applications and materials capable of producing tens of thousands, up to a hundred thousand photons per 1 MeV incident radiation (ph/MeV) have been developed. ILY of a scintillator can be approximated in ph/MeV as:

$$\text{ILY} \approx \left[\frac{10^6}{\beta E_g}\right] S \times \text{QE} , \qquad \text{(Eq. 2)}$$

where S characterises the transfer efficiency of electron-hole pairs to the luminescence center, QE is the quantum efficiency of the luminescence center, β is a constant and E_g the energy gap of the material. Factor βE_g expresses the average energy required to produce one thermalized electron-hole pair and is generally in

the order of 2–3 times of the energy gap value. It is clear that materials with smaller energy gap values are therefore more efficient scintillators. However, high ILY is useful for improving time resolution of fast timing applications only if the photons are emitted in a time frame corresponding to the targeted time resolution. This can be expressed by density of photons and is in first approximation given by ILY/τ_d, but as it is discussed below, for novel fast timing applications also rise time τ_r must be considered.

Short decay times are possible for emissions resulting from optically allowed electronic transitions. Current top of the line TOF-PET systems (*e.g.,* Siemens Biograph Vision) use Lu_2SiO_5:Ce^{3+} (LSO) crystals as its scintillator material. The Ce^{3+} 5d → 4f transitions are parity and spin-allowed and the emission has a decay time of 40 ns. LSO's short decay time and high light yield of 25 000 ph/MeV lead to a CTR value of 160 ps. Short decay times are also observed for cross-luminescence (below 1 ns, discussed in detail in the next section) and for intrinsic emissions that are strongly quenched (6 ns for $PbWO_4$ at room temperature, used in the CMS calorimeter in CERN).

Emission rise time can be excluded from the emission decay model only if it is negligible compared to emission decay time [5]. This is not the case for scintillators developed for novel high-end timing applications and emission rise time has a profound effect on the overall time resolution performance of the detection system. Moreover, fundamental limits of ILY and τ_d have been nearly reached with standard scintillators [6]. Optimising the processes that affect emission rise time have been defined as one of the main challenges in achieving the high design goals set for novel fast timing scintillators [2].

Emission rise time is dependent on a series of relaxation processes taking place between the initial interaction of high-energy radiation quanta or particles with scintillator material and the activation of luminescent centres where scintillation light is eventually emitted [7]. First, in the time scale of 10^{-16} to 10^{-14} s, deep holes in the inner core bands and hot electrons in the conduction band are created by incident high-energy radiation. Thereafter, secondary electronic excitations are produced by inelastic electron-electron (e-e) scattering and Auger processes. Then, as a second step in time scale 10^{-14} to 10^{-12} s, after kinetic energy of electron in the conduction band has decreased below the threshold of e-e scattering ($< 2E_g$) and the electrons are therefore unable to further ionize the material, thermalization of electronic excitations begins by electron – phonon scattering. At the end of this process, low kinetic energy, thermalized electrons populate the bottom of the conduction band and holes the top of the valence band. In the third step (10^{-12} to 10^{-10} s) of the process, the excitations are localized through interaction with stable impurities and defects of the material, electrons and holes can be trapped or self-trapped. Excitons, self-trapped excitons (STE), self-trapped holes (V_K centres) are formed. Fourth and the final step takes place in a time scale of 10^{-10} to 10^{-8} s and is related to slow migration of relaxed excitations and eventually their non-radiative or radiative recombination, the latter resulting in scintillation photons.

The above described processes are fundamentally stochastic and create statistical fluctuations in the creation of first, *i.e.,* prompt scintillation photons, increasing emission rise time and consequently reducing the time resolution of the detector. The intrinsic fluctuations in creation of prompt photons can be estimated to be in the order of 100 ps. In order to achieve the 10 ps CTR goal set for future TOF applications, an alternative approach has been proposed [8]. This involves the detection of radiative processes of non-thermalized charge carriers, taking place in a time scale of 1 picosecond from the excitation. The properties of intraband luminescence (IBL) and Cherenkov radiation, which meet such requirements, will be discussed in detail in the next section.

While several general requirements must be met for scintillator materials to be used in practice, materials for novel high-end timing applications must in addition possess short emission decay and rise times and high photon density (ILY/τ_d) as discussed earlier. Intrinsic processes leading to such favourable properties will be discussed below.

Overview of intrinsic processes leading to ultrafast emission

Cross-luminescence

Cross-luminescence (CL) is an intrinsic emission resulting from the radiative recombination of a relaxed core hole with an electron from the valence band [9]. The process in energetically allowed only if the energy distance between the top of the valence band and the outermost core level is less than the energy gap ($E_{VC} < E_g$), otherwise Auger decay will take place. The origin of CL was clarified in the early 1980s [10] and extensively studied during 1990s in several materials (see review [11] and references therein) as a scintillation process potentially suitable for fast timing applications. CL was initially revealed in binary alkali and alkali-earth fluorides (BaF_2, KF, RbF) and caesium salts (CsBr, CsCl, CsF), but later also in multi-component materials based on these binary compounds [9]. The main interest in using CL materials in fast timing applications is based on its emission decay times in sub-ns to ns scale. The decay time for CL in BaF_2 has been measured to be 0.92 ns under 30 eV synchrotron radiation excitation, while even shorter decay times were observed at higher excitation energies due to quenching [12]. BaF_2 is probably the most studied CL material because of its favourable properties, which include fast decay time, relatively high light yield compared with other CL materials (1700 ph/MeV [13]), physical density (4.88 g/cm^3) and chemical stability. BaF_2 was initially studied in the 1970s as a scintillator because of its slow 320 nm STE emission, before fast CL was discovered (220 nm), making it the fastest known scintillator in use at the time. More recently, it has been shown that BaF_2 single crystal can be used to achieve a CTR of ~ 80 ps with photodetectors based on modern silicon-photomultipliers (SiPM) [3, 14]. Another significant advantage of CL is thermal stability, as the process only involves electronic excitations in the outermost core level and valence band,

between which competitive non-radiative processes are suppressed due to their energetic separation. It has been shown that no thermal quenching occurs in BaF_2 and CsCl up to 750 K [15]. Disadvantages of materials with CL include low light yield compared to established scintillators and emissions mostly occurring in the ultraviolet (UV) and vacuum ultraviolet (VUV) spectral region, making detection technically challenging with common photodetectors operating in vacuum conditions. Among binary CL materials mentioned above, only CsF emits in a more favourable spectral region peaking at 390 nm, but is unfortunately also very hygroscopic as known for Cs-salts generally.

The problem of unfavourable emission spectral position can be mitigated by considering more complex compounds based on the classical binary CL materials. Valence band structure of many ternary compounds is more complex, consisting of multiple sub-bands due to the splitting of electronic states and thus providing more possibilities for radiative transitions between the outermost core band and the valence sub-bands [16]. The fast emissions in ternary CL compounds are shifted into the UV [17] and also into visible spectral region as shown by the results of this work. Also, splitting of the valence band creates favourable conditions for increased IBL yield, a phenomenon further discussed in the next section.

Recent research using the band structure engineering approach combined with modern experimental methods, supported by the development of novel photodetectors based on SiPMs with increased detection efficiency in the UV region has helped CL regain its status as a process involved in the development of scintillators to be used in high-end timing applications [2].

Intraband luminescence

IBL is a weak emission originating from radiative transitions of electrons and holes during the thermalization stage [18–21]. It is a characteristic luminescence to all solids and has a wide emission spectrum spanning over the whole transparency region of the material. IBL intensity is not dependent on temperature, impurity content nor crystal structure quality. Decay time of IBL is in the general case estimated to be in the order of 1 ps while light yield is estimated to be in the order of 10^{-5} to 10^{-3} per electron-hole pair [8]. However, while these figures are true for materials with uniform density of states (DOS) distribution in the valence and conduction bands, some materials host a more complex distribution, which can result in increased light yields and decay times. Dips and gaps in the DOS cause accumulation of charge carriers above the structures and radiative transitions become more prominent compared to non-radiative phonon-assisted transitions. Thus, such modulations in the DOS distribution can result in IBL light yields in the order of 10^{-3} with 1 ps decay times for dips, while gaps can further increase this value to 10^{-2} with 100 ps decay times expected [8]. Experimentally the yield of IBL has been estimated to be 33 ph/MeV for CsI pure crystal in the highest case [22], which is low, in comparison with scintillators in use, but it can be sufficient to use these few IBL prompt photons as time taggers in high-end timing applications.

Cherenkov radiation

Another phenomenon that could produce prompt photons to be used for time tagging with essentially non-existent delay is Cherenkov light. It is produced in scintillators when hot electrons created by high-energy incident radiation travel at speeds greater than the speed of light in that material. Cherenkov radiation is similar and could be indistinguishable from IBL at excitation energies above the Cherenkov threshold, typically in the 100 to 300 keV range. A material applied as a Cherenkov light emitter is PbF_2, suitable for this purpose because it has high gamma radiation stopping power, good transmittance of Cherenkov light, does not scintillate and is also a low-cost material. CTR figures below 100 ps have been achieved for Cherenkov emitters in experiments using MCP-PMTs as photodetectors [2].

Nano-scintillators used for fast timing applications

A fundamentally different approach is considered when developing nano-scintillators for fast timing applications. With nano-crystals, the opto-electronic properties of the scintillator can be controlled by the geometry and size of the particle. Nano-platelets with 1-dimentional quantum confinement of charge carriers provide ultrafast emissions with higher light yields than Cherenkov or IBL. A concept using hybrid pixels has been implemented, in which a known inorganic scintillator (*e.g.,* LYSO, BGO) is combined with nano-crystal-based layers [23]. In this combination, prompt photons from the nano-crystal are added to the standard scintillation signal, effectively improving the time resolution.

Band structure engineering approach

Research and development of scintillator materials is driven by the needs of the corresponding industries [1]. The needs have over time become increasingly specific, leading to development of complex scintillators. A systematic approach of band structure engineering is used to produce the desired properties sought in novel scintillators. It combines first-principle computation of electronic properties with state of the art experimental methods to gain detailed knowledge about the features of the band structure and relaxation processes of electronic excitations. Based on the obtained knowledge, the host material can be further modified with the introduction of impurity ions and/or isovalent substitution of a part of the host ions with formation of solid solutions. Using this approach, the scintillator properties of materials can be fine-tuned to match the needs of the target application.

Novel detectors for fast timing applications

This work is focused on scintillator properties, however an important role in the time resolution of an ionizing radiation detector is also carried by the photo-detector and its readout electronics. Purpose of the photo-detector is to convert light signal from the scintillator into an electrical signal, which can then be digitalised and in timing applications a time stamp of the arrival of the signal is stored. Naturally, some amount of delay is associated with this process and fluctuations in the delay (*i.e.,* jitter) reduce the time resolution of the whole system.

Nowadays SiPMs are considered as the successor of classical photomultiplier tubes as photo-detectors in various applications including TOF-PET. SiPMs are compact, acquire a considerably lower bias voltage and cost less to produce, to name some of the advantages over photomultiplier tubes. Important parameters in describing the time resolution performance of a SiPM are the photon detection efficiency (PDE) and single photon time resolution, directly related to the ability of a detector to time stamp prompt photons [24]. The development of SiPMs has also resulted in increased PDE in the UV and VUV spectral region [25], where most of the cross-luminescence emissions in binary compounds are situated. For example, on an experimental setup using SiPMs as photodetectors and BaF_2 as a scintillator, CTR of ~ 80 ps has been achieved [3]. Matching the luminescence signal properties of scintillators to current photo-detectors and *vice versa* improving photo-detectors for more efficient detection of ultrafast emissions from novel scintillators will lead to overall improved time resolution of the whole system.

3. FORMULATION OF THE RESEARCH GOAL AND SPECIFIC SUBTASKS

The main objective of this PhD work is to provide the research field of inorganic scintillators with new and detailed knowledge on the intrinsic luminescence properties of new scintillator materials to be exploited in fast timing applications. The objective includes specification of underlying relaxation mechanisms in materials possessing cross-luminescence and intraband luminescence. In order to achieve this objective, the following research tasks were established and completed:

- Applying band structure engineering approach to improve luminescence properties of materials with known ultrafast emissions such as cross-luminescence and intraband luminescence.

- Identifying new potential scintillator materials with desirable properties based on computational properties and electronic band structures. Successfully synthesizing samples of the materials for luminescence studies.

- Studying emissions in new scintillator materials using sophisticated experimental techniques at state-of-the-art large-scale synchrotron radiation research facilities, achieving superior time resolution and gaining in-depth knowledge by means of time-resolved luminescence spectroscopy.

- Developing a state-of-the-art time-resolved luminescence setup for studies of ultrafast emission at LINAC based FemtoMAX beamline, its implementation and performing commissioning research.

- Analysing the origin and behaviour of ultrafast cross-luminescence and intraband luminescence emissions revealed, combining experimental and computational research results.

4. DESCRIPTION OF RESEARCH METHODOLOGY

Syntheses and materials properties characterization

Powder samples of the materials studied were synthesized at our home institute in Tartu implementing soft chemistry methods.

In synthesis of K_2SiF_6, the initial reagents included KF (Sigma-Sigma-Aldrich, 99.5% purity), tetraethyl orthosilicate (TEOS, Sigma-Aldrich, 98% purity), HF (Sigma-Aldrich, 40 vol.% water solution, reagent grade), ammonia (Sigma-Aldrich, 30 vol.% water solution, reagent grade), all without any further purification [26]. TEOS was hydrolysed via standard ammonia-catalysed reaction in water-alcohol solution to obtain SiO_2, which was then precipitated out and dried. The acquired SiO_2 powder was dissolved in HF solution, to which a stoichiometric amount of KF was added under vigorous stirring. The mixture was treated in a microwave-hydrothermal device for 2 hours at 180 °C, centrifuged, washed with distilled water and dried.
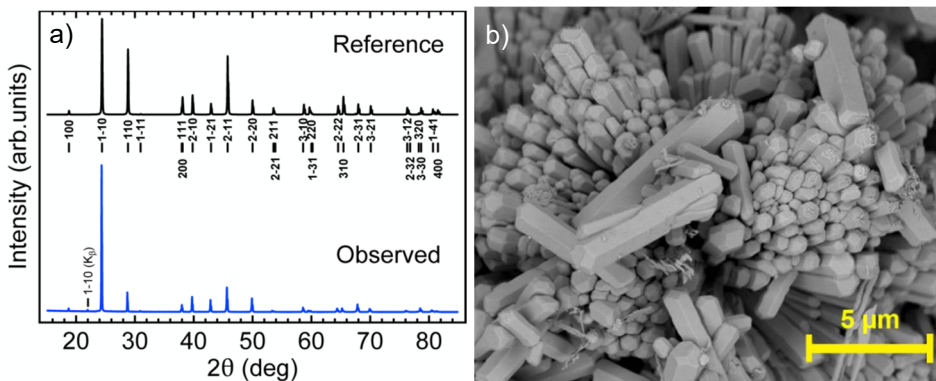

Figure 1. (a) Observed XRD patterns of the synthesized powder (lower panel) and reference pattern (upper panel) of trigonal $BaGeF_6$ from the ICDD database (PDF-2 file number 74-0924). Miller indices and positions of reflections of the trigonal $BaGeF_6$ are shown below the reference pattern. (b) SEM micrographs of obtained $BaGeF_6$ micropowder particles.

In order to synthesize $BaGeF_6$, initial reagents used included $Ba(NO_3)_2$ (Sigma-Aldrich, >99.9% purity), GeO_2 (Reakhim, reagent grade) and HF (Sigma-Aldrich, 40 vol.% water solution, reagent grade) without further purification. The synthesis first involved dissolving GeO_2 in HF and then diluting the result with water, forming a water solution of H_2GeF_6. $Ba(NO_3)_2$ was dissolved in water and then stirred into the H_2GeF_6 solution. The resulting reaction mixture was then sealed into a Teflon autoclave and heat-treated in an oven for 24 hours at 150 °C. The mixture was then centrifuged, washed using alcohol and dried in air at 100 °C.

The initial reagents used to synthesize K_2GeF_6, without any further purification, included KOH (Sigma-Aldrich, > 99.5% purity), GeO_2 (Reakhim, reagent grade), HF (Sigma-Aldrich, 40 vol.% water solution, reagent grade), and methanol

(Sigma-Aldrich, technical grade). KOH was dissolved in a minimal amount of deionized water and stirred into a H_2GeF_6 water-alcohol solution, prepared in parallel by mixing GeO_2, HF and methanol. The resulting mixture was stirred vigorously for 24 hours and then centrifuged. The resulting powder was washed with alcohol and dried at 100 °C in air.

X-ray diffraction (XRD) method using a 8.1 kW source (Cu K_α radiation, λ = 0.1540598 nm) and Bragg-Brentano optics on a SmartLab™ X-ray diffractometer (Rigaku, Japan) was used to analyse the phase composition of the synthesized samples (Figure 1a as an example). Furthermore, scanning electron microscopy (SEM), using a NanoSem 450 (FEI) microscope at voltages below 5 kV without a charge reduction layer, was used to study the morphology of the microparticles (Figure 1b). XRD and SEM studies were carried out at our home institute in Tartu.

Cathodoluminescence studies

Cathodoluminescence studies under electron beam excitation were conducted at our home institute in Tartu using two custom setups.

First one of the setups is equipped with an electron gun (Kimball Physics EGG-3101) producing either a steady beam of 10 keV electrons or 10 ns pulses at 5 kHz repetition rate [27]. This setup is equipped with two monochromators – an ARC Spectra Pro 2300i for recording spectra in the UV to visible range (6–1.8 eV) with multiple available gratings for different spectral ranges, coupled with a Hamamatsu photon counting head H8259. The second one is based on a custom built, double grating vacuum monochromator for recording spectra in the VUV spectral range (photon energies up to ~11.2 eV), using a solar-blind Hamamatsu R6836 photomultiplier. These monochromators were used with the spectral resolution as high as 0.5 and 0.64 nm, respectively, and can simultaneously record luminescence spectra in the separate spectral ranges. The setup is equipped with a closed cycle helium cryostat ARS (Advanced Research System, Inc.) providing temperature control in the 5 to 400 K range.

The second cathodoluminescence setup is designed for recording time-resolved emission spectra and decay kinetics in a wide energy and temperature range [28]. The electron gun (RADAN-303A SFEE) can provide electron pulses in an energy range of 100–200 keV with excitation pulse width as short as 40 ps at 5 Hz repetition rate. The samples are mounted on a cold finger of a helium closed cycle cryostat ARS (Advanced Research System, Inc.), which allows temperature control in the range of 7 to 400 K. The setup is also equipped with two luminescence detection systems operating in the 0.8–5.7 eV and 4–10.8 eV photon energy ranges, respectively. Measurements in the low energy range can be conducted by utilizing an Andor Shamrock SR303i spectrograph coupled with a Hamamatsu R3809U-50 MCP-PMT (nominal transit time spread 25 ps) mounted at the exit slit of the spectrograph and a position sensitive Andor iStar DH 720_18 mm gated iCCD camera mounted on the imaging port. The second detection system for the VUV range is comprised of a custom designed Seya-

Namioka type vacuum monochromator with 1200 g/mm gold-coated grating blazed at 160 nm and a Hamamatsu R3809U-58 MCP-PMT. The signal from the MCP-PMT detector is amplified by an SHF 100 APP broadband preamplifier (12 GHz, 19 dB) and digitized by a LeCroy SDA 760Zi-A (6 GHz, 40 Gs/s) oscilloscope with 50 Ω input. The IRF of this setup has been measured to be as excellent as 60 ps FWHM. The spectral sensitivity of the detection systems has been calibrated in the whole spectral region using response known crystals (*e.g.*, LYSO:Ce), allowing for estimation of light yields of ultrafast emissions below 50 ph/MeV, based on a method described in detail in [22].

Photoluminescence studies using synchrotron radiation

Photoluminescence studies using synchrotron radiation as an excitation source were carried out at the FinEstBeAMS beamline's photoluminescence endstation (PLES) at the MAX IV laboratory in Lund, Sweden. FinEstBeAMS is an Estonian-Finnish beamline for atmospheric and materials science at the MAX IV 1.5 GeV storage ring [30–32]. FinEstBeAMS radiation source is an elliptically polarizing undulator (Figure 2, EPU) providing high brilliance radiation in the UV to soft X-ray range of 4.5 to 1300 eV with photon flux in the range of 1×10^{11} to 8×10^{13} ph/s.
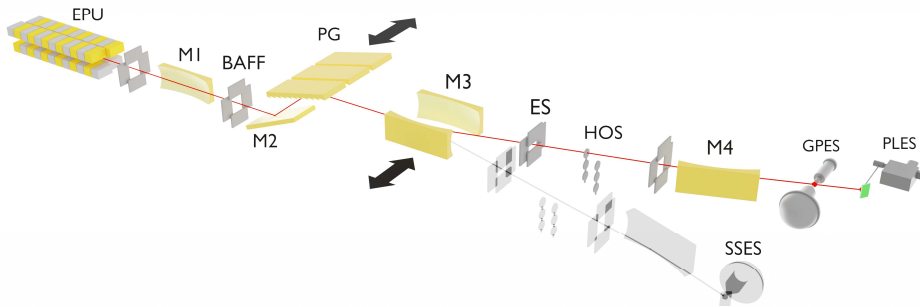

Figure 2. Layout of the FinEstBeAMS beamline's optical system and endstations. EPU – elliptically polarizing undulator; M1-M4 – mirrors; BAFF – baffles; PG – plane gratings; ES – entrance slit; HOS – higher-order suppression unit; GPES – gas-phase endstation; SSES – solid-state endstation; PLES – photoluminescence endstation. Courtesy of Dr. K. Chernenko [32].

The first optical element of the beamline, a toroidal mirror (M1) collimates the beam and directs it to the input of a grazing incidence primary monochromator equipped with two Au-coated plane gratings (PG) – 92 l/mm and 600 l/mm groove density, exploited to provide excitation photon energies in 4.5 to 50 eV and 15 to 1300 eV range, respectively. All measurements in the current work were performed using the 92 l/mm grating. A set of toroidal mirrors (M3) allow to select one of the two beamline branches providing photon beam to different

endstations of the beamline and to focus the beam to the exit slit (ES). The latter is followed by a higher-order suppression unit (HOS) where a set of optical windows (fused silica, MgF_2) and metal foils (In, Sn, Mg, Al) are available for higher order radiation suppression at photon energies below 72 eV. As the last optical element, an ellipsoidal mirror (M4) refocuses the radiation into a 100×100 μm spot onto the PLES sample holder mounted on a cold finger of a closed-cycle helium cryostat ARS (Advanced Research System, Inc.). Experiments are conducted under ultra-high vacuum conditions.

Luminescence emitted from the sample is collected using a metal-shielded fibre-optic cable and directed to the input of an Andor Shamrock SR-303i spectrometer. The spectrometer is equipped with three gratings (blazed at 300, 500 and 1200 nm) and a set of optical longpass filters for higher order suppression. For detection, an Andor Newton DU970P-BVF CCD camera is mounted on one of the output ports of the spectrometer while either a Hamamatsu H8259-01 photon counting head or a Hamamatsu R3809U-50 MCP-PMT (used to achieve sub-ns time resolution) is mounted on the second one, depending on the aim of the experiment. Typical spectral resolution used in the recording of the luminescence spectra on this setup was 12 nm. Generally, the 1.5 GeV storage ring operates in multi-bunch mode, in which 32 electron bunches travel in the storage ring with a nominal current of 500 mA, topped up periodically from the MAX IV LINAC. The time distance between bunches is 10 ns, amounting to a total period of 320 ns for a single electron bunch to travel one full circle of the storage ring. Recording time-resolved spectra and decay kinetics in multi-bunch mode would be feasible only if the emissions measured have a lifetime less than 10 ns, which is the case for the ultrafast emissions discussed in this work. However, there is often some amount of slow emissions from samples present at the studied wavelengths and this creates a slow background in the 10 ns measurement window because of their long decay time, which may cover the ultrafast emission components entirely. In order to allow more time for the slower emissions to decay – to be fully de-excited, the measurements can be conducted in the storage ring's single-bunch operation mode. In this mode, a single electron bunch is travelling in the storage ring instead of the 32, therefore providing a 320 ns time interval between the excitation pulses, a time window that can be used to record luminescence decay kinetics. In single-bunch mode, the bunch length is less than 200 ps, while exceeding 450 ps in multi-bunch mode according to our studies. Single-bunch mode is available only at certain periods and the excitation intensity is lower than in multi-bunch mode (ca 20 times less current), which affects the data collection time to have reasonable SNR.

Time-resolved studies were conducted under the single-bunch excitation implementing a special timing method developed and implemented by us [33]. Time-resolved emission and excitation spectra as well as single decay kinetics can be recorded at FinEstBeAMS. For luminescence detection, the ultrafast R3809U-50 MCP-PMT was used and signal was processed by an ORTEC 9327 1 GHz preamplifier – constant fraction discriminator and timed by a Cronologic xTDC4 time-to-digital converter with 13.0208333 ps bin width. Modern

time-to-digital analysers allow for detection of multiple emission photons from a single excitation pulse. We performed full decay analysis of a number of emission and excitation spectra, meaning the recording of single decay kinetics in a range of emission wavelengths and excitation energies, respectively. The method results in time-resolved spectra that can be divided into time windows based on the lifetime of the emissions observed. Temporal resolution as fine as 143 ps (FWHM of a Gaussian fit of the measured IRF) was achieved with this setup, limited by the excitation pulse (electron bunch) length. Throughout this work, decay kinetics analysis was performed taking into account the measured IRF by applying deconvolution to fit the decay curves in order to obtain reliable results.

The fibre-optic cable used to direct luminescence to the spectrometer poses some technical problems in recording of emission spectra. Poor transmission of the fibre-optic cable below 250 nm decreases emission intensity and also creates difficulties in acquiring reliable calibration lamp spectra needed to correct the emission spectra for spectral sensitivity of the setup. Sensitivity correction is further complicated due to non-linear dependencies between emission intensities in the UV region and the primary slit width. Emission spectra in this work are therefore presented as measured, *i.e.*, on wavelength scale, if not indicated differently. Also, a detection time difference is created between photons of different energies due to the fibre-optic cable's wavelength-dependent refractive index, which is corrected using an equation created on the basis of time-resolved experimental data.

Higher order harmonics radiation is always created in the undulator and can pass through the primary monochromator operating in grazing incidence geometry. Optical windows (fused silica, MgF_2) and metal thin film filters (In, Sn, Mg, Al) are used to suppress higher order radiation in different excitation energy ranges up to 72 eV. Excitation spectra in broad excitation energy ranges were recorded using several different filters and treated taking into account the significant differences in their transmission (from few % to tens of %).

Future experiments will be performed at a new photoluminescence beamline P66 on PETRA storage ring at DESY, Hamburg. P66 is a bending magnet beamline providing excitation energies from 4 to 40 eV from a normal incidence primary monochromator equipped with Al and Pt coated gratings. Normal incidence geometry suppresses higher orders with the help of low Al and Pt reflection coefficients above 20 and 40 eV photon energies, respectively. The beamline has also two separate detection systems, one for visible to UV range emissions and a vacuum monochromator for VUV emission measurements.

Ultrahigh time resolution studies excited by X-ray pulses

FemtoMAX is a beamline located at the Short-pulse facility (SPF) at the MAX IV laboratory (Lund, Sweden) and is driven directly by the LINAC (3 GeV) [34]. FemtoMAX aims to facilitate studies of the structure and dynamics of materials, providing very short and intense X-ray excitation pulses along with synchronized laser impulses for pump and probe experiments. FemtoMAX currently generates hard X-ray photons pulses shorter than 200 fs from 1.8 to 12 keV, at 10 Hz repetition rate. This makes the beamline also well suited for experiments of ultrafast luminescence processes by simulating real operation conditions of scintillators.

A special experimental setup was designed, assembled and tested for studies at FemtoMAX, with specific aim to achieve efficient luminescence detection of low intensity emissions without compromising time resolution. The experimental chamber is a DN 100 CF 5-way cross mounted on a custom levelling plate (Figure 3).
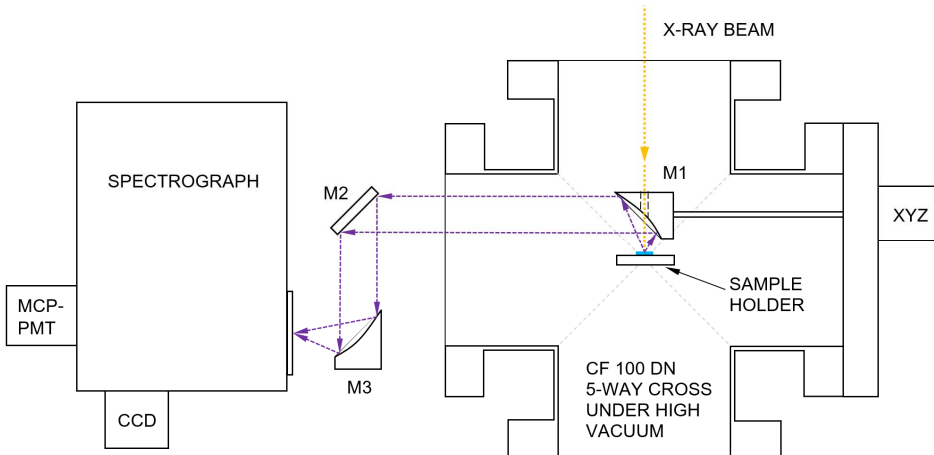

Figure 3. Schematic of the experimental setup built for luminescence experiments at the FemtoMAX beamline. M1 and M3 are off-axis parabolic mirrors and M2 is a plane mirror. XYZ indicates a XYZ manipulator controlling mirror M1 position. Sample holder is attached to the cold finger of the LNT cryostat.

A Janis VPF-800 liquid nitrogen cryostat with a sample holder is mounted on the top port of the cross, allowing to use temperatures starting from 78 K up to 800 K in high vacuum conditions. A one inch (25.4 mm) focal distance off-axis parabolic mirror M1 (Thorlabs, Inc.) is mounted in front of the sample holder with its focal spot on the sample to collect luminescence light. The mirror has a through hole (Ø 4.1 mm) perpendicular to the focal plane and the sample holder. The exciting X-ray beam (ca 120 × 120 µm) enters the experimental chamber from the front port and propagates through the hole in the M1 mirror onto the sample. The parabolic mirror M1 is attached to a XYZ manipulator mounted on one of the side ports of experimental chamber. The mirror collects luminescence light

from the sample and directs it as a parallel beam (under 90° relative to the incident exciting X-ray beam), towards the second side port of the experimental chamber with a CF35 fused silica optical window. Backside port of the experimental chamber has a CF100 glass window used for monitoring and alignment purposes and is capped during experiments to reduce scattered light level, which could disturb measurements. The parallel beam of light outside the experimental chamber is directed onto a second off-axis parabolic mirror M3 (focal distance 76.2 mm) using a plane mirror M2, if needed. The second parabolic mirror M3 focuses the incoming parallel beam either directly to a photocathode of a detector or an input slit of a spectrometer. The spectrometer and detector exploited in the experiments at FemtoMAX were an Andor Shamrock SR-303i (from FinEstBeAMS) equipped with a Hamamatsu R3809U-50 MCP-PMT (also used at the single bunch experiments at FinEstBeAMS), respectively. Signal from the MCP-PMT was amplified by a SHF 100 APP broadband preamplifier (12 GHz, 19 dB) and digitized by a FemtoMAX local LeCroy LabMaster 10-36Zi oscilloscope (36 GHz, 80 Gs/s). The signal was then further processed by advanced multi photon counting technique, which allows the detection of several non-overlapping luminescence photons per single excitation pulse. A special LabView software was developed by us in order to perform this task. The time resolution achieved with this setup was as excellent as 32 ps (FWHM of IRF Gaussian fit), limited by the time resolution of the MCP-PMT. A detailed description and comparison of the time-resolved luminescence spectroscopy experimental setups and beamlines at MAX IV and DESY can be found in [35].

5. RESEARCH RESULTS AND DISCUSSION

Examples of classical cross-luminescence in BaF₂

As briefly discussed above, BaF_2 is one of the most studied CL materials. Recently, interest in exploiting intrinsic emissions of this scintillator material has increased. Conducted research has revealed some promising results in achieved CTR, implementing a detection system based on BaF_2 crystals in combination with novel SiPMs [14]. In this work, BaF_2 was mainly studied as a scintillator crystal with known emission properties and high CL light yield. The results obtained allowed to compare and validate the new experimental setups and methods developed in this work. Furthermore, the improved time resolution in sub nano second range can be helpful in studies of ultrafast relaxation processes and reveal decay components of ≤ 100 ps duration.

BaF₂ crystal was studied at the FinEstBeAMS beamline's PLES, where integral emission spectra under excitation by 50 and 17 eV photons were recorded (Figure 4). The spectrum recorded under 50 eV photon excitation comprises mainly of two non-elementary emission bands, peaking at 219 and 300 nm. The bands are known intrinsic emissions of BaF_2, the 219 nm emission is due to cross-luminescence resulting from radiative recombination of valence electrons with Ba 5p core holes (Ba 5p → F 2p) [10].
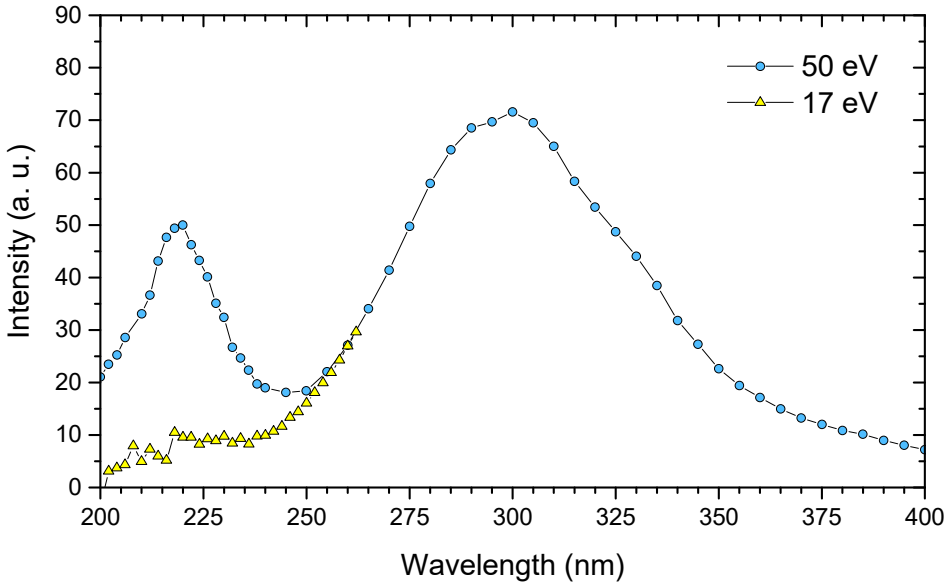

Figure 4. Emission spectrum of a BaF₂ crystal at 7 K, recorded under excitation by 50 eV (blue circles) and 17 eV (yellow triangles) photons at the FinEstBeAMS beamline. The emission spectra were corrected to transmission of detection channel and sensitivity of photodetector. Mg and Sn filters were applied to remove higher order radiation at the respective excitation energies.

The band peaked at 300 nm is due to triplet self-trapped exciton (STE) emission with a life-time of 630 ns at room temperature (296 K), whereas for CL the life-time is 0.9 ns (see [36] and references therein). The emission spectrum recorded under 17 eV photon excitation does not show any luminescence peak at 219 nm, being in agreement with the known threshold of 18.2 eV for CL luminescence excitation in BaF_2 [37]. There is some residual luminescence observed, which emerges from "white soft X-ray background" and cannot be suppressed by any metal filter available at FinEstBeAMS. The spectra also demonstrate the tremendous possibilities of using highly selective photoexcitation in materials research.

A decay curve of CL from a BaF_2 single crystal recorded at the FinEstBeAMS beamline is shown in Figure 5a. The curve was recorded through a 216 nm interference filter during an excitation scan from 18 to 23 eV photons at 7 K under ultra-high vacuum conditions. Similarly, the same interference filter was used to record a CL decay curve of BaF_2 at the FemtoMAX beamline under 10 keV X-ray excitation at room temperature (Figure 5b) in a sample chamber at ambient pressure during the first test beamtime for luminescence studies at FemtoMAX. The curves were fitted with two- and three-component exponential decay functions, yielding similar results in decay constants. The IRFs shown on the figures illustrate well the time resolution of the experimental setups compared to each other. Under VUV excitation, two decay components were identified at 7 K.
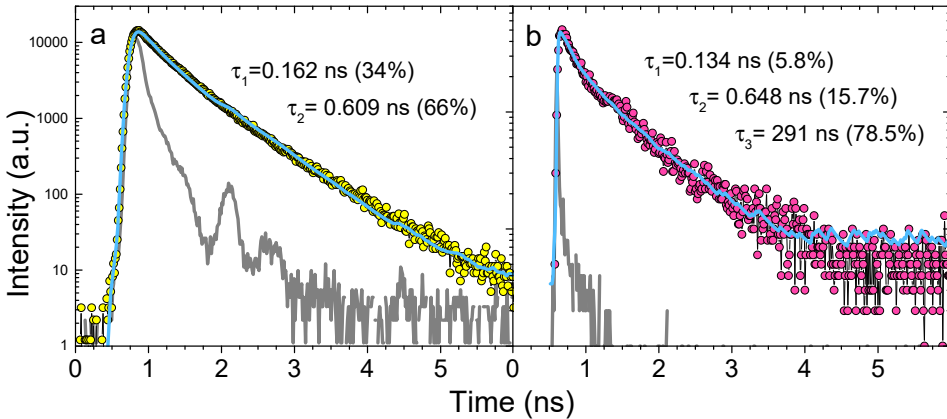

Figure 5. Decay curves of cross-luminescence for a BaF_2 crystal recorded through a 216 nm interference filter (IF216): (a) at 7 K under excitation by 18–23 eV photon pulses (~ 160 ps; with the Sn filter applied) at the FinEstBeAMS and (b) at 296 K excited by 10 keV pulses shorter than 200 fs at the FemtoMAX. The decay curves were fitted with the exponential decay functions (solid blue lines) by deconvolution with the corresponding IRFs and the obtained decay times together with their relative integral intensities are shown in the graphs. Very different IRFs are shown for both setups with a solid grey line with FWHM values of 160 ps and 28 ps. The same ultrafast MCP-PMT was used as a photodetector in both experiments.

The first one τ_1=163 ps coincides with the IRF value 160 ps, whereas the second component τ_2=609 ps is shorter than the 920 ps reported in [12] under analogous conditions. The study conducted at FemtoMAX at 296 K using excitation by 10 keV photon pulses shorter than 200 fs, revealed that the fastest component is τ_1=134 ps, followed by τ_2=648 ps, which is comparable with that under VUV excitation. The IF216 filter transmission extends up to 300 nm, covering the short wavelength part of STE emission (Figure 4). Decay time of the third component is τ_3=291 ns. This result demonstrates that the time resolution provided by storage rings is not sufficient for studying decays in the sub nanosecond range, but it can be performed at the LINAC-based sources like FemtoMAX at MAX IV Lab and FLASH at DESY, where properties of BaF_2 scintillator under high density excitation in XUV were studied [38].

BaF_2 crystal with 1% La doping was studied at the FemtoMAX beamline using the advanced experimental setup developed by us and described in detail above. Figure 6 shows the decay curves of CL from a BaF_2:La 1% crystal recorded through the spectrometer for 225 nm emission at 295 and 80 K. Thus, only CL is detected without any disturbing influence of STE emission.
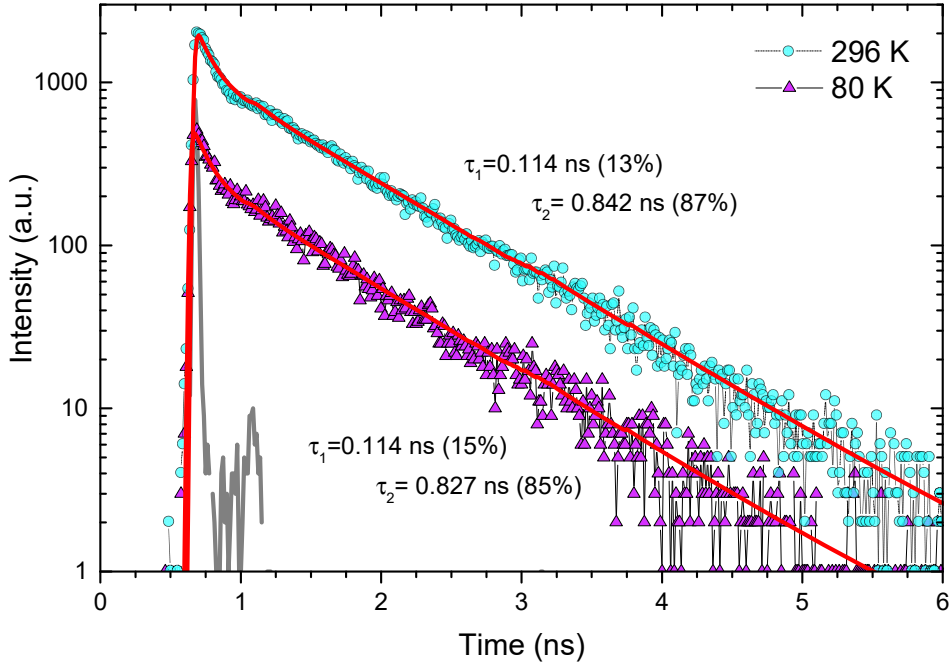

Figure 6. Decay curves of CL at 225 nm (spectrally selected by a monochromator with 5.4 and 10.8 nm spectral resolution at 296 and 80 K, respectively) excited by 10 keV photon pulses shorter than 200 fs at the FemtoMAX beamline. The decay curves were fitted with a two-component exponential decay functions (red lines) by deconvolution based on the IRF with 32 ps FWHM (solid grey line). The decay time values are also shown alongside with their relative integral intensities.

It is well known that CL intensity and decay times have no temperature dependence [9], which is also confirmed by our experiments. A two exponential fit for decays at both temperatures results in an ultrafast component τ_1=114 ps and τ_2=827 and 842 ps, respectively. The second component in La doped BaF_2 is slightly longer in comparison with the CL decay (~ 600 ps) in pure BaF_2. Very similar decay time values have been reported for BaF_2:La 1% under 511 keV photon excitation and using a VUV-SPAD for detection [14]. Based on this solid experimental result, we can firmly state that there is an ultrafast decay component, which has to be taken into account in describing relaxation processes of core excitations in materials with cross-luminescence. This, however, is beyond the scope of present work.

The decay curves can be well approximated with a sum of two exponentials pointing to the fact there are no non-linear phenomena observed, which are due to mutual interaction of dense core excitations. Using experimental parameters like 120×120 μm^2 spot size on sample, amount of photons $1.5*10^6$ ph/pulse and literature data for absorption of 10 keV photons in BaF_2, the estimated core excitations density is $\leq 5*10^{15}$ cm^{-3}, which is low enough to be in a linear excitation regime without a distortion of decay kinetics, as confirmed by the experimental results. Strong non-exponential dependence of decays has been observed for various scintillators under high-density excitation in experiments performed at FLASH [38].

Considerable amount of time was spent to record the decay curves acquired at the FemtoMAX beamline. This is due to the combination of low excitation repetition rate available (10 Hz) and the applied multiple photon counting method. The method is capable of detecting and timestamping multiple emission photons per excitation pulse, but if the photons are detected too close to each other to be accurately timestamped, the respective information is discarded. Therefore, contrary to the general case in luminescence measurements, relatively low luminescence intensity is needed to record a data in optimal time. Parameters used to optimise this are the percentage of excitation impulses, which are not discarded due to overlapping impulses (*i.e.*, percentage of good shots) and the average number of detected photons per excitation pulse. For example, in case of the decay curves presented in Figure 6, the parameter values were ca 60% good shots and 0.6 photons detected per excitation pulse. Data integration time due to 10 Hz repetition rate was about 9 h for the decay curve measured at 295 K and 2 h for the decay curve measured at 80 K, which explains the significant difference in peak intensities of decays shown in Figure 6.

Electronic properties of synthesized ternary fluorides

The ternary fluoride powders synthesized in this work all have a complex valence bands, according to theoretical electronic band structure calculations (*e.g.*, see public AFLOW database [39]). Main band structure parameters deduced from experimental data of the measurements performed in this work, with other properties from literature for the studied compounds are shown in Table 1.

Table 1. Properties of studied ternary fluorides. Energy gap (E_g) and cation energy gap (E_{gc}) values were deduced from features revealed in the experimental excitation spectra of the respective emissions. Density values taken from the AFLOW database [39]. * unpublished results.

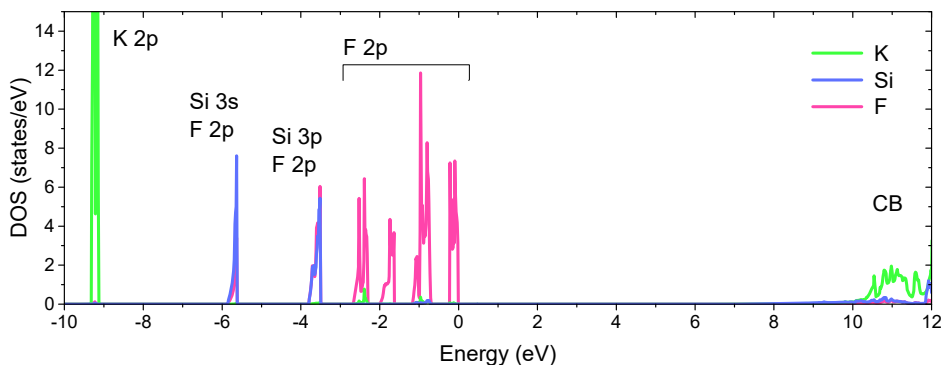| Compound	E_g (eV)	E_{gc} (eV)	Density (g/cm^3)	Reference
K_2GeF_6	11.0	20.0	3.23	[33]
$BaGeF_6$	10.9	19.4	4.60	[40]
K_2SiF_6	10.6 *	~ 20.0 *	2.62	
Na_2GeF_6	~ 12.0 *	~ 34.0 *	3.02	

Figure 7. DOS distribution for K_2SiF_6. From left to right – outermost core level comprised of K 2p states (solid green line); split valence band hybridised states comprised of Si 3s, 3p (solid blue line) and F 2p states (solid magenta line); conduction band (CB). Data from AFLOW [39].

In this section, the band structure properties of K_2SiF_6 are discussed as an example for ternary fluorides. Outermost core level in K_2SiF_6 is comprised of nearly pure K 2p states (Figure 7). Valence electronic states of K_2SiF_6 are formed by the hybridized fluoroanion SiF_6^{-2} bands [16]. Nearly pure F 2p valence states form four well-separated bands in the energy range 0 to –2.5 eV and hybridised Si 3s – F 2p and Si 3p – F 2p states in energy range –2.5 eV to –6 eV form all together a rather complex band structure. These hybridised bands are energetically positioned in the gap between the F 2p valence band and K 2p core states. Energy distance between the outermost core level and the top of the valence band is smaller than the energy gap E_g values, allowing for radiative transitions resulting

in CL between the core level and valence band states like in binary compounds with CL [9]. Furthermore, with the introduction of Si, the gap between the core level and valence band has significantly decreased, compared to the parent binary KF, creating conditions for a possible red shift of the CL emissions. The presence of split valence states due F 2p, Si 3p and Si 3s can introduce a rich emission spectrum due to intraband transitions covering the energy range up to 5.9 eV (energy difference between F 2p and Si 3s positions). The distinct gaps between valence bands can influence properties of ultrafast IBL, namely increase the light yield and characteristic decay times, as discussed in [8]. These properties of ternary hexafluorides may lead to using the IBL prompt photons as time taggers.

Interpretation of ultrafast emissions and their decay times

In order to achieve the objective of current PhD thesis and to explain the nature of observed emissions, sophisticated analysis of the experimental results was carried out. The complexity of calculated valence band structure for ternary $BaGeF_6$ hexafluoride is shown in Figure 8, alongside with the revealed ultrafast emissions resulting from radiative transitions between the states of composing elements. In this figure, the observed ultrafast emissions from $BaGeF_6$ are directly connected to the transitions between different states of the core and valence bands. Figure 8a shows the computational band structure of $BaGeF_6$ taken from the AFLOW repository [39], while Figure 8b shows emission spectra of $BaGeF_6$, combined from time-resolved PL emission spectrum recorded in a 0–3 ns time window (below 6 eV) and time-integrated cathodoluminescence emission spectrum above 5.7 eV, which extends to VUV range. The coloured boxes drawn in Figure 8b relate the corresponding radiative transitions marked with letters a. to f., to the arrows with same notation in Figure 8a. The starting position in the energy scale and width of a box in Figure 8b is defined by the onset energy of the corresponding emission (minimal energy distance between the states involved, shown in Figure 8a) and the maximal energy width of the target band involved. Coincidence of the computational data and experimental results is evident. The detailed analysis of the emissions illustrated in this figure has been carried out and reported in [40]. Such analysis is shown to be a very useful tool for other ternary hexafluorides studied and is a prime example of the role of the band structure engineering approach, which has been implemented in preparation of modified materials in this work.

Resulting ultrafast emissions in ternary hexafluorides with analogous complex band structure are often due to a combination of CL and IBL and recorded decay curves of the overlapping emissions tend to show nature of CL and IBL. However, in Na_2GeF_6 the Na 2p cation electronic states lie much deeper at –18.7 eV in respect to top of valence band. Its valence band comprised of GeF_6^{-2} fluoro-anion states is split into sub-bands. Therefore, IBL transitions are still possible between the split valence band states, but the energetic condition for CL is not fulfilled and ionization of Na 2p core level results in a decay of a core hole through Auger process with electron emission.
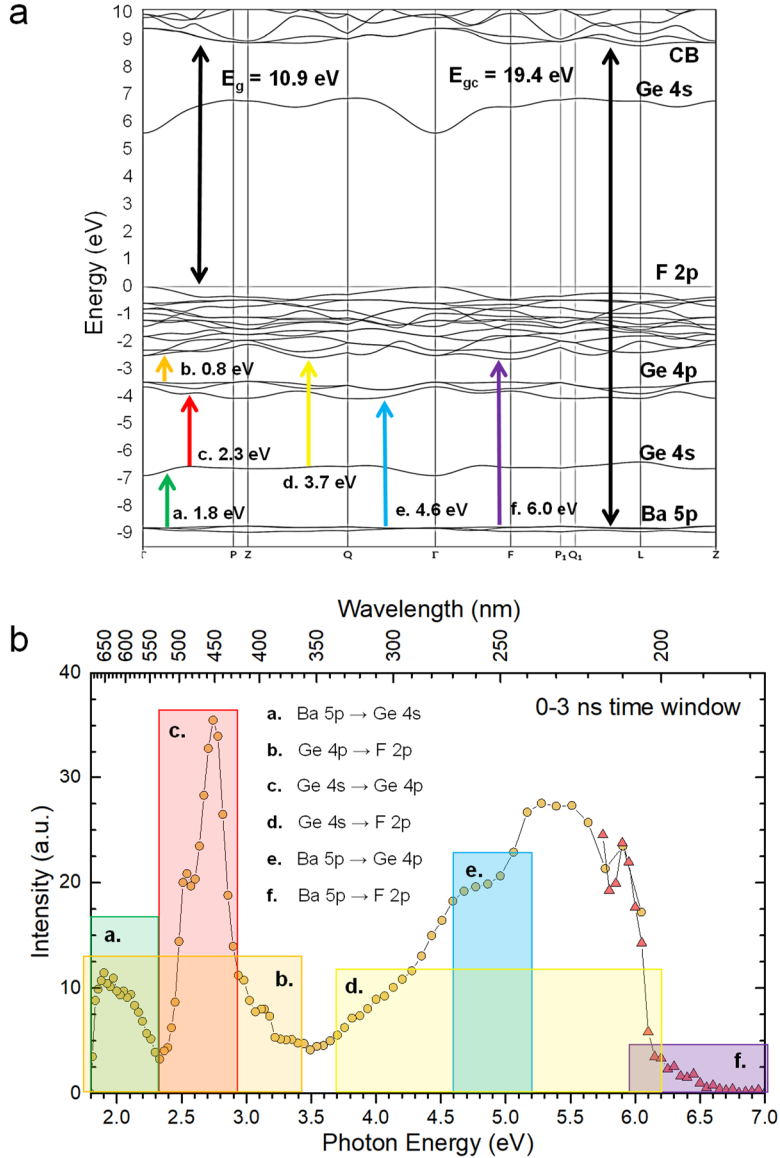
Figure 8. (a) Computational electronic band structure of BaGeF$_6$ [39] with the experimental energy gap (E$_g$) and energy distance between the outermost core band and conduction band (E$_{gc}$) shown. (b) PL emission spectra of BaGeF$_6$ at 7 K in a 0–3 ns time window (UV-Vis, circles) excited by 45 eV photons combined with cathodoluminescence emission spectra in the VUV region (> 5.7 eV, triangles). The boxes in panel (b) indicate radiative transitions (a.-f.) with relevant energy of onset (minimal calculated energy distance between the bands involved, also shown in panel (a)) and width (target band energy width).
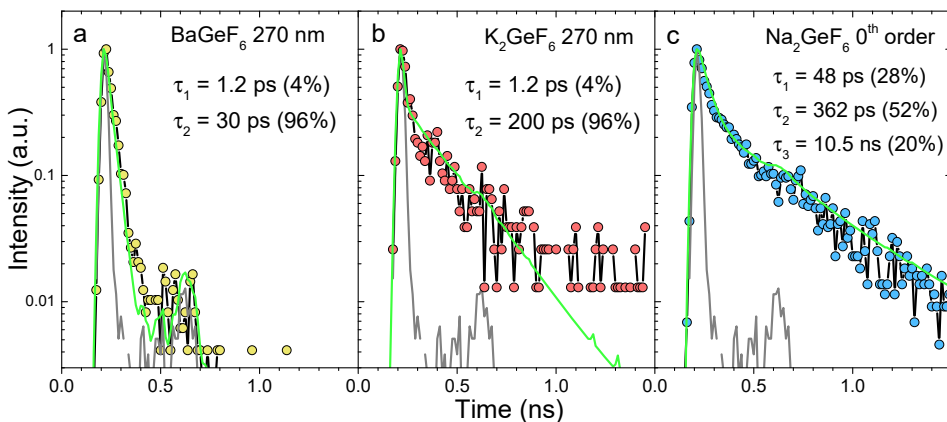
29

Figure 9. Decay curves for various ultrafast emissions from ternary hexafluorides at 80 K excited by 10 keV photon pulses shorter than 200 fs at the FemtoMAX beamline. a) 270 nm emission of $BaGeF_6$; b) 270 nm emission of K_2GeF_6 (τ_2 was fixed to 200 ps); c) 0th order *i.e.,* spectrally integrated luminescence emission of Na_2GeF_6. IRF of the detection system is shown in a solid grey line. The decay curves were fitted with exponential decay functions (solid green lines) by deconvolution with the corresponding IRF and the obtained decay times together with their relative integral intensities are shown in the graphs.

Figure 9 shows decay curves for various ultrafast emissions from ternary hexafluoride powders at 295 K. The experiments were performed at the FemtoMAX beamline and decays were recorded through a monochromator at well-defined emission wavelengths with 27 nm spectral resolution. The decays are very short in the sub nanosecond time domain, which is typical for materials with CL and IBL. Ultrafast emissions observed in Na_2GeF_6 were very weak most likely due to absence of CL contribution and the decay was consequently recorded as a spectrally integrated one by setting the analysing monochromator into "zeroth" order. Data analysis showed that depending on the complexity of the decay curves, multi-exponential fitting function resulted in the best approximation. Statistical data quality varies from sample to sample and is mostly limited by the amount of beam time available. The statistically best IRF was recorded from $BaGeF_6$ powder at room temperature for 270 nm emission resulting in 32 ps value. This result was verified by IBL decay at 270 nm recorded from a Li_2MoO_4 crystal, which has previously also been used to obtain IRF [23], but did not yield a statistically valid result this time as scintillation yield of the emission measured through a monochromator was too low.

Data analysis by multi-exponential fit of decay curves for various hexafluorides showed that there is always a very short component present in order of 1 ps, which cannot be considered as a physically realistic decay at the current experimental conditions. 270 nm emission (4.6 ± 0.21 eV) in $BaGeF_6$ (Figure 9a) is IBL due to overlapping Ba 5p → Ge 4p and Ge 4s → F 2p transitions (see Figure 8 and [40]). Thus, the main component for this emission has a decay time

$\tau = 30$ ps and its relative integral contribution is 96 %. It agrees surprisingly well with the theoretical prediction that IBL decay times may reach tens of pico-seconds in case of a split energy band structures [8]. The experimental data was not so favourable for 270 nm (4.6 ± 0.21 eV) emission in K_2GeF_6 as the fit did not converge properly due to low statistics. The line shown in Figure 9b is drawn for a decay with a characteristic time of $\tau = 200$ ps, illustrating the expected rate of the processes. According to the energy band structure, 270 nm emission in K_2GeF_6 is due to intraband luminescence transition Ge 4s $\rightarrow$ F 2p [33]. In case of Na_2GeF_6, spectrally resolved studies of decays could not be performed due to weak lumi-nescence intensity. Tri-exponential fit resulted in the following decay times: $\tau_1 = 48$ ps (its relative contribution 28 %), $\tau_2 = 363$ ps (52 %) and $\tau_3 = 10.5$ ns (20%). The first component is tentatively assigned to IBL between split valence band states (F 2p, Ge 4s and 4p) because it is more unlikely that the conduction band has gaps in the density of states. The second decay component is in the decay time range of CL, which cannot take place in Na_2GeF_6 because Na 2p cation core level is located too deep at ~ -18.7 eV and Auger decay takes place. The third identified component has a life-time, which typical for some allowed electronic transitions. In order to perform detailed analysis of emission spectra in Na_2GeF_6, additional spectroscopic studies are required.

Scintillation yield of hexafluorides

Scintillation yield of the studied ternary hexafluorides was estimated using a special method devised by us for low light yield scintillation processes, *e.g.*, for IBL with light yield values below 50 ph/MeV [22]. The scintillation yield values estimated for the ultrafast emissions of the powder samples of $BaGeF_6$, K_2GeF_6 and K_2SiF_6 were 4.5, 4.0 and 25 ph/MeV, respectively. The estimation method only takes into account the ultrafast emissions and contribution from slower emissions is not considered, which is generally not the case for scintillation yields reported elsewhere. It is also important to point out that the light yield estimation was carried out for powder samples, which typically show smaller yields in comparison to single crystals. There has been progress in growing single crystals of some ternary hexafluorides in our group, but these studies will be carried out in future.

The higher light yield of K_2SiF_6 could be the influence of fully split F 2p valence states, increasing the yield of IBL in comparison to other hexafluorides. According to the band structure calculations, the distribution of F 2p valence states in $BaGeF_6$ and K_2GeF_6 is more smooth without well-distinguished gaps in DOS. Slightly higher yield of $BaGeF_6$ is probably due to the heavier Ba cation, which shortens radiation length and increases energy losses. Scintillation yield of Na_2GeF_6 was not estimated but it is expected to be lower than in the other germanates as there is no CL and also because of the comparatively lower inten-sity observed during luminescence experiments. CL does not undergo thermal quenching [15], but electron-phonon interaction definitely influences the IBL yield. It will be discussed in the forthcoming sections.

Temperature dependence of electronic excitations
in ternary fluorides

Temperature is an important variable in studies of optical and luminescence properties of solids. Low temperature studies allow suppressing of the non-radiative decay channels, which quite often quench the radiative decay of intrinsic electronic excitations at room temperature. Important information on heights of activation barriers can also be deduced from studies of temperature dependence of various phenomena as well as performing spectroscopic studies in the temperature ranges, where delocalization of charge carriers takes place, influencing energy transfer processes [41].

Room and low temperature emissions in K_2GeF_6 and $BaGeF_6$

Cathodoluminescence emission spectra of synthesized K_2GeF_6 and $BaGeF_6$ powders were recorded at room (295 K) and low (5.5 K) temperatures under excitation by 10 keV steady electron beam (Figure 10 and Figure 11). The luminescence spectra were simultaneously recorded in the VUV and UV-visible range with separate monochromators and the results obtained overlap in the 200–275 nm region. Although unusual, it was chosen here to present the cathodoluminescence spectra in wavelength scale to simplify comparison with other spectra presented in this work recorded under synchrotron radiation excitation.

Low temperature emission spectra of $BaGeF_6$ powder show two broad emission bands peaking at around 225 and 455 nm (Figure 10). The bands both have a complex structure comprising of several different emissions. The band peaking at 225 nm is also evident in the recorded VUV spectrum, but in this case, the SNR of the data is not ideal and is affected by lower sensitivity of the detection system in this spectral region. The band peaking at 225 nm has been shown to be CL and the broad band peaking at 455 nm has been assigned to self-trapped exciton emission of μs duration by us [40]. Room temperature spectra of the same sample are significantly different. The broad emission band peaking at 455 nm is substituted by two elementary emissions peaking at 355 and 555 nm, which are most probably of extrinsic origin. It must be considered that luminescence spectra above 600 nm are influenced by second order contribution from emissions in UV. The 225 nm CL emission band is observable in the spectrum recorded at room temperature at a similarly low intensity as it is at low temperature, but absolute intensities of the spectra are not comparable in this case as the experimental parameters were not completely identical.

Low temperature cathodoluminescence spectrum of K_2GeF_6 shows also multiple emission bands covering the whole studied spectral range (Figure 11). It is important to note that all luminescence spectra in VUV were recorded in time integrated mode under electron beam excitation in the home laboratory because there were no spectrometers available for VUV luminescence detection at synchrotron radiation centres.
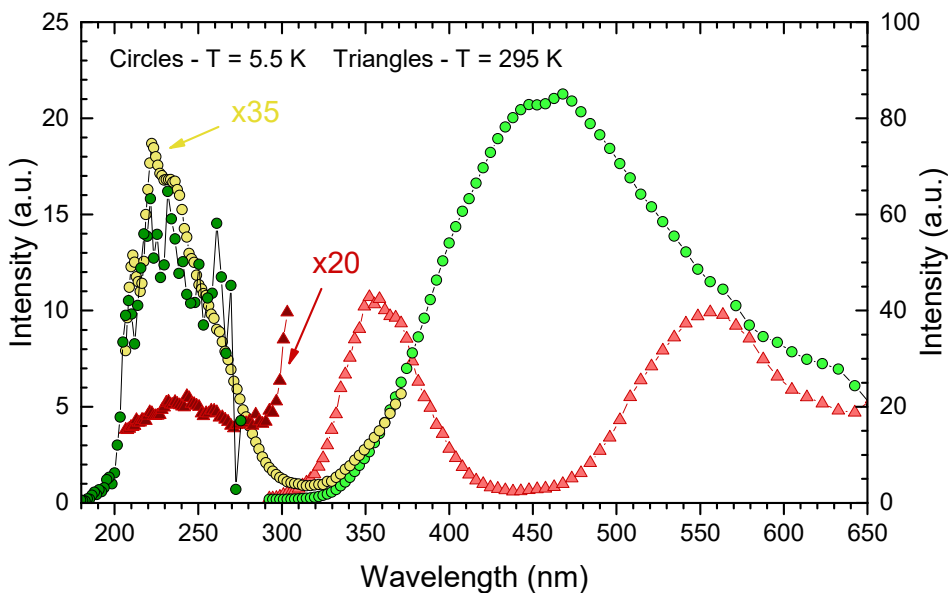
Figure 10. Cathodoluminescence emission spectra of $BaGeF_6$ recorded at 295 K (red triangles) and 5.5 K (green circles) under 10 keV electron beam excitation. Spectra recorded in the 200–300 nm region are multiplied by a factor of 35 for better visualization. The spectra were corrected for the spectral sensitivity of the detection system.
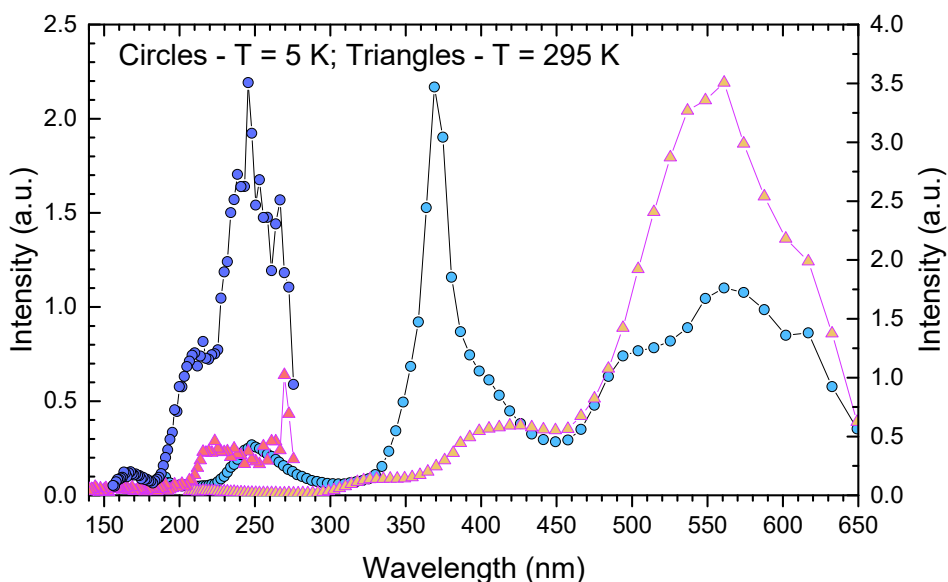

Figure 11. Cathodoluminescence emission spectra of K_2GeF_6 recorded at 295 K (pink triangles) and 5 K (blue circles) under 10 keV electron beam excitation. The spectra were corrected for the spectral sensitivity of the detection system.

In the short wavelength VUV region starting from 150 nm, multiple emission peaks are observed, forming a broad band of low-intensity emissions, which are already assigned to CL from the time-resolved photoluminescence experiments above 200 nm conducted by us at FinEstBeAMS [33]. Low temperature emissions at wavelengths above 300 nm are somewhat different from the ones observed under photoexcitation using SR, where a single broad band peaked at 510 nm was observed. Obviously, energy transfer processes exciting all possible luminescence centres are more pronounced under electron beam than applying more selective photoexcitation resulting in population of particular single luminescence centre. Meanwhile room temperature cathodoluminescence emission spectrum in this region features multiple peaks in the 300 to 650 nm region, matching well with unpublished results from the recent time-resolved photoluminescence studies by us. In this region, the origin of emissions is mixed – a contribution from ultrafast emissions is observed in the 400–450 nm spectral region, while the other peaks are slow emissions of µs duration most probably from STE formation as shown in [33].

Temperature dependence of slow emissions in BaGeF$_6$

Temperature dependence of the broad visible emission of BaGeF$_6$ powder was studied using pulsed and steady-beam cathodoluminescence setups in the Institute of Physics in Tartu (Figure 12). Decay of the 480 nm emission was recorded in 5.4 – 300 K temperature range using pulsed 200 keV electron beam excitation.
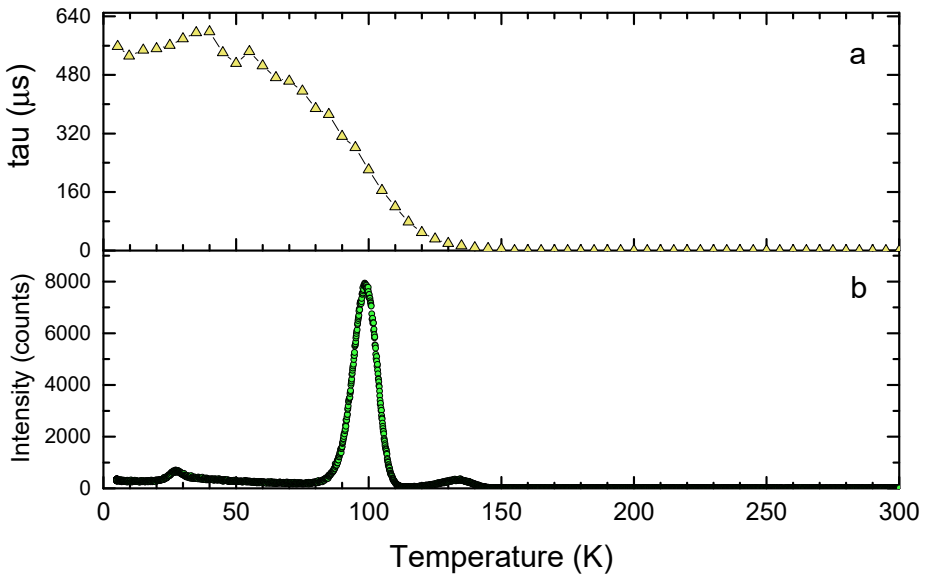

Figure 12. a) Temperature dependence of the slow µs decay component for 480 nm emission from BaGeF$_6$ powder, recorded under 200 keV pulsed electron beam excitation; b) TSL spectrum of BaGeF$_6$ for 434 nm emission through UV-visible monochromator after 10 keV electron beam irradiation at 5 K.

In data analysis, the decays were fitted with an exponential decay function resulting in temperature dependence of the decay constant as shown in Figure 12a. At low temperatures, value of the decay constant is ~560 µs, which starts to decrease above 40 K, followed by its rapid shortening and eventually, as can be seen in Figure 12a, the 480 nm emission is quenched at 130 K. This is characteristic behaviour of intrinsic emissions in wide gap materials and strongly supports that this emission is due to STE as assigned in [40]. Figure 12b features a thermally stimulated luminescence (TSL) spectrum recorded for 480 nm emission from $BaGeF_6$ powder after irradiation by 10 keV electron beam at the other cathodoluminescence setup. There are a few TSL peaks revealed at 30, 98 and 130 K. The prominent TSL peak at 98 K represents a temperature range where delocalisation of charge carriers (self-trapped holes) can occur, resulting in disintegration of STEs and the related emission is thermally quenched. Although the two temperature dependences presented in Figure 12 were studied at two different setups, the shortening of decay times and the appearance of the prominent TSL peak is well correlated and 480 nm is related to STE luminescence.

Thermal quenching of ultrafast emissions

High temperature stability of CL in binary BaF_2 and CsCl has been demonstrated up to temperatures of 750 K [15] and also demonstrated in this work for CL decays in BaF_2 in the temperature range of T=80–300 K in Figure 6. The temperature dependence of ultrafast emissions in ternary hexafluorides seems to be more complex than that of CL in binary compounds. A comparison of time-resolved emission spectra from K_2GeF_6 powder at 296 and 7 K excited by 45 eV photons at FinEstBeAMS in shown in Figure 13. The spectra were recorded in a time window of 0–3 ns and absolute intensities of the spectra are comparable as experimental parameters were identical. The spectra have not been corrected for sensitivity of the detection system and transmission of optical path due to reasons discussed in the research methodology section in detail. Ultrafast emissions revealed in the spectra are a combination of CL and IBL, similarly to what was described above for $BaGeF_6$ in Figure 8. Origin of the emissions is analysed in detail in [33]. The main spectral features remain similar in whole temperature range studied, but intensity of ultrafast emissions at 296 K is lower all across the spectral region. As classical CL does not depend on temperature as reported in [15], current results show that there are some processes present leading to the reduced luminescence intensity of ultrafast emissions, most likely thermal quenching of IBL due to increased electron-phonon scattering rate. In the case of CL, the phonon interaction controls the thermalization rate of charge carriers, but does not influence electron-hole recombination resulting in CL.
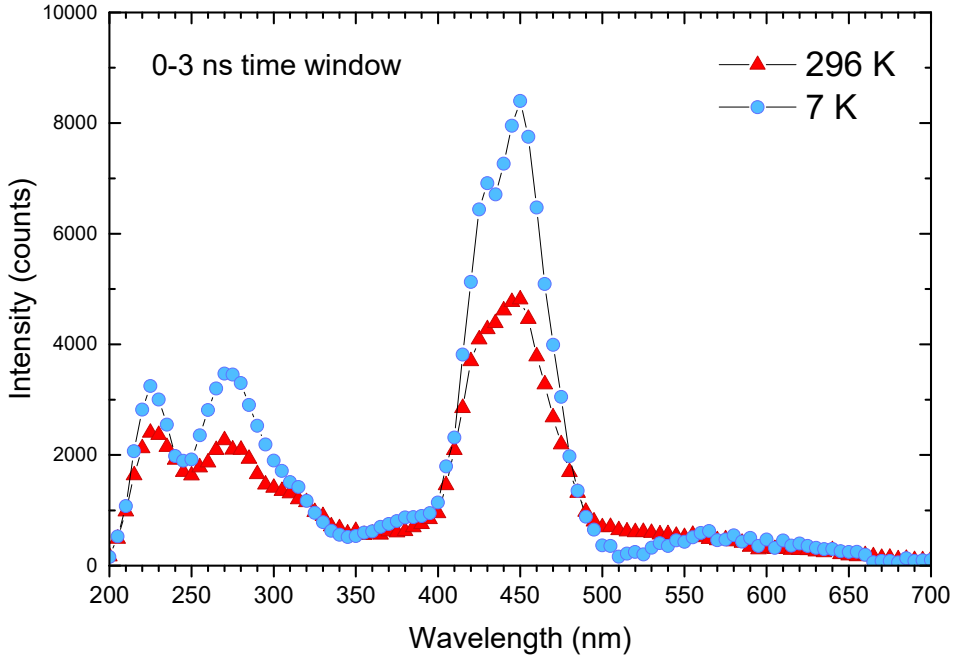
Figure 13. Time-resolved emission spectra of the ultrafast emissions (recorded in a time window of 0–3 ns duration) of K_2GeF_6 powder recorded under 45 eV photon excitation at 296 K (red triangles) and 7 K (blue circles) using the FinEstBeAMS beamline. The spectra were recorded using identical experimental parameters.

In order to learn more about the thermal quenching processes, temperature dependence of ultrafast emissions of K_2GeF_6 powder was investigated for 225 and 430 nm bands using pulsed 200 keV electron beam excitation. Obtained decay curves were fitted with an exponential decay function resulting in temperature dependence of the decay constant and initial amplitude as shown in Figure 14. Since these ultrafast components are rather weak emissions, the statistical quality of data acquired at a satisfactory level has resulted in somewhat scattered curves, but still good enough for converging numerical values. One can see that decay times of both emissions behave in a similar way in the temperature range of 5–300 K: for 225 nm the decay time decreases a little from 0.25 to 0.2 ns and for 430 nm somewhat more from 0.29 to 0.13 ns. The change in amplitudes follows a similar declining trend as initial amplitudes of both emissions decrease. The amplitude of the 225 nm emission band shows a strong consistent decline from 1.85 to 0.23 units. For the 430 nm emission, the amplitude decreases from an initial 1.46 to 0.59 units.
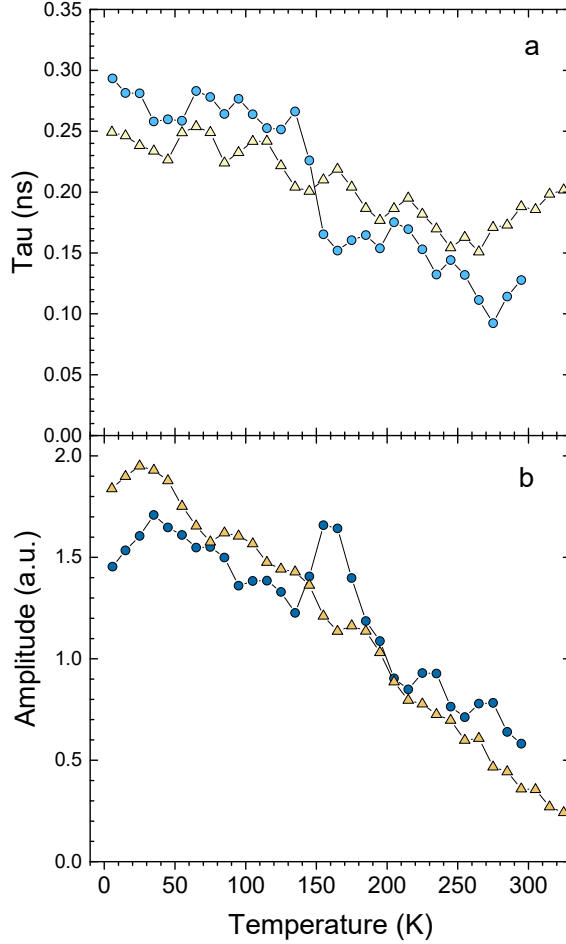
Figure 14. Temperature dependence of ultrafast emissions from K_2GeF_6 powder, recorded at 225 nm (yellow triangles) and 430 nm (blue circles). a) Temperature dependence of the emission decay time; b) Temperature dependence of the emission amplitude obtained from fitting of the decay data.

Temperature dependence of the 430 nm emission band has a notable decline for decay time at 135 K, matched with a steep increase of its amplitude. This effect in most probably related to the increased intensity of slow background STE emission, covering the ultrafast component and increasing amplitude through the whole decay time range. Temperature quenching of IBL in ternary hexafluorides could be due to the split valence band structure. The yield and decay time of IBL is dependent on the structure, gaps increase IBL yield and decay times can become longer [8]. According to the theoretical calculations in Materials Projects, phonon energies in K_2GeF_6 are up to 75 meV [42]. This facilitates crossing energy gaps by influence of phonons up to 5 times of a maximum phonon energy *i.e.,* up to 375 meV. This gives an indication that the population of Ge 4s, 4p states and Si 4s, 4p states should be quite stable (see Figure 7, 8 and [33, 40]). However, the

population of F 2p states forming the valence band undergoes relaxation due to phonons because the energy gaps are practically absent (BaGeF$_6$, K$_2$GeF$_6$) or in the range of the five phonon energies (K$_2$SiF$_6$). Temperature influences the population of charge carriers in the split valence band states, which can therefore lead to redistribution of occupied DOS, resulting in different thermal quenching of IBL bands of different origin in ternary hexafluorides. Figure 13 indicates that UV emissions are slightly less influenced by temperature than the emission peaked at 450 nm. There is an overlap with slow STE peaked at 520 nm and thermal quenching of STE at 295 K has also an influence. Further studies of this phenomenon are required to confirm this and give detailed explanation to the thermal quenching of IBL.

6. CONCLUSIONS

In this thesis, luminescence and optical properties of $BaGeF_6$, K_2GeF_6, K_2SiF_6 and Na_2GeF_6 micropowder samples and BaF_2 and BaF_2:La 1% single crystals were investigated using time-resolved luminescence spectroscopy at room and low temperatures under electron beam and synchrotron radiation excitation. Time-resolved studies were used to record emission and excitation spectra, decays for various emissions and their temperature dependencies were studied on different experimental setups. Ternary hexafluoride samples synthesized by soft chemistry methods were characterized using XRD, SEM and other methods to get information on crystallite size, phase composition and morphology of samples under investigation.

The main results from the thesis are summarized in a general level below:

- Band structure engineering approach was successfully applied in the design and synthesis of hexafluoride micropowder samples.

- It was shown that in case of studied ternary hexafluorides, cross-luminescence can be successfully shifted into the UV – visible spectral range by applying band structure engineering approach in materials design.

- Important band structure parameters like energy gap and cation energy gap were experimentally determined for the studied ternary hexafluorides.

- The revealed and extensively studied ultrafast emissions with sub nanosecond decay time are assigned to cross-luminescence due to transitions between outermost core band and complex valence band states formed from hybridized fluoroanion bands and intraband luminescence due to transitions between the split valence band states.

- Thermal quenching of ultrafast emissions in the studied ternary hexafluorides is most likely due to redistribution of the density of valence states affecting the yield and decay times of intraband luminescence.

- Scintillation yield of ultrafast emissions observed in the powder samples was relatively low, but is expected to be considerably higher for single crystals.

- Ultrafast luminescence in BaF_2 and BaF_2:La crystals consists of known fast cross-luminescence component and in case of BaF_2:La, an additional, even faster second decay component.

- A new mobile experimental setup specifically for time-resolved studies in sub nanosecond time range was developed and launched at the FemtoMAX beamline driven directly by the LINAC at the MAX IV Laboratory, achieving time resolution as excellent as 32 ps (IRF FWHM).

- It was shown that the achievable time resolution of storage ring based beamlines is sufficient for studies of relaxation processes of electronic excitations (160 ps IRF FWHM at FinEstBeAMS operating at the 1.5 GeV ring at MAX IV), but not high enough for the precise characterisation of decay times of ultrafast intrinsic emissions in scintillators.

Future research directions of ultrafast emissions in ternary hexafluorides and other complex compounds include syntheses and characterisation of samples in single crystal form. Scintillation properties of single crystals are expected to be better than in micropowder samples. Improved scintillation properties allow to study the involved processes at a more detailed level, as well as allow to evaluate the potential practical use of the compound more accurately in real scintillation conditions.

In order to gain further knowledge about the underlying relaxation processes leading to ultrafast emissions, time resolved studies with at least an order of magnitude higher time resolution are needed. Pump and probe experiments based on upconversion luminescence method under free-electron laser and X-ray free-electron laser excitation can provide time resolutions in sub-ps range. Such research will elucidate in detailed way, *i.e.* spectrally and in fs time domain, ultrafast energy transfer and relaxation processes in scintillators based on intrinsic emissions.

Time-resolved studies of visible to VUV range emissions under highly selective photoexcitation can be conducted at the P66 beamline of the Petra III storage ring at DESY (Hamburg, Germany). A combination of monochromators covering the UV-visible and VUV spectral range allows to study the ultrafast emissions of ternary hexafluorides in their full spectral range of luminescence.

7. SUMMARY

Scintillator materials with specific luminescence properties are needed in a wide range of applications in medicine, high energy physics, homeland security and elsewhere. Band structure engineering approach is a method of combining computational band structure data with experimental results to achieve the desired properties in new scintillator materials.

Ternary hexafluorides were identified as potential new scintillator materials to be used in fast timing applications based on the known luminescence properties of their binary counterparts and computational electronic band structures. A hypothesis was formed that the complex valence band structure of the materials split into several separate sub-bands potentially allowed for a multitude of ultrafast radiative transitions and a red shift of cross-luminescence emissions.

Micropowder samples were successfully synthesized and their phase purity confirmed using XRD analysis and morphology visualized using SEM imaging. The samples were then characterized using several different luminescence spectroscopy methods, acquiring in-depth knowledge about the luminescence and optical properties of the materials. Key experiments in this work were time-resolved luminescence studies conducted under pulsed electron and synchrotron radiation excitation. A custom experimental setup for time resolved studies was developed and an outstanding time resolution of 32 ps was achieved.

Origin of the intrinsic emissions revealed was thoroughly analysed. Ultrafast emissions with sub 500 ps decay times were revealed in all of the compounds, extending from VUV to visible spectral range. In the analysis of the experimental time-resolved emission and excitation spectra, the computational band structure data was used to attribute the emissions to cross-luminescence and intraband luminescence. It was demonstrated that ternary hexafluoride systems based on the known binary cross-luminescence materials can provide ultrafast luminescence emissions shifted to the UV and visible spectral region, making a detection of the ultrafast luminescence feasible by modern ultrafast silicon-photomultipliers.

Current work demonstrates that band structure engineering approach can be efficiently used by combining the potential of modern computational methods with state-of-the-art experimental studies for the design of novel scintillator materials with targeted electronic and luminescence properties.

8. SUMMARY IN ESTONIAN

Ülikiirete relaksatsiooniprotsesside uurimine kolmekomponendilistes heksafluoriidides sünkrotronkiirguse ergastusel

Erinevates kõrgtehnoloogilistes rakendustes meditsiinis, teaduses ja julgeoleku vallas esineb vajadus spetsiifiliste luminestsentsomadustega stsintillaatorite järele. Kõrget ajalist lahutusvõimet vajavatesse rakendustesse otsitakse stsintillaatoreid, mis tekitaks neeldunud kõrg-energeetilise ergastuse mõjul viiteta ja võimalikult lühikese pikalainelise valgusimpulsi. Kross-luminestsents ja tsoonisisene luminestsents on tahkistes esinevad omakiirgused, millel on ülilühike kustumisaeg, kuid mille saagis on madal. Lisaks asuvad kross-luminestsentsi kiirgused enamasti VUV–UV lühilainelises spektriosas, kus fotodetektorite tundlikkus on madalam. Doktoritöö eesmärgiks oli rakendada tsoonistruktuuri modifitseerimise lähenemist (ingl k *band structure engineering*) nende puuduste leevendamiseks, kombineerides arvutuslikke tsoonistruktuuri andmeid eksperimentaalsete uuringutulemustega.

Tuginedes kahekomponendiliste fluoriidide (KF, BaF_2 jt) teada olevatele luminestsentsomadustele ja arvutuslikele tsoonistruktuuri andmetele leiti, et kolmekomponendiliste heksafluoriidide näol võiks tegu olla potentsiaalsete uute stsintillaatoritega, mida kasutatakse kõrge ajalise lahutusvõimega rakendustes. Kolmanda elemendi (Ge, Si) lisamisega moodustub kompleksne valentsitsooni struktuur, mis on jaotunud eraldiseisvateks alamtsoonideks (F seisundid ning hübridiseerinud Ge-F või Si-F seisundid). Näidati, et heksafluoriidides on võimalikud mitmed ülikiired kiirguslikud üleminekud nii kõige kõrgemate katioonseisundite ja valentsitsooni alamtsoonide vahel (kross-luminestsents) kui ka tsoonisisesed kiirguslikud üleminekud valentsitsoonis sees (tsoonisisene luminestsents). Väiksem vahekaugus katiooni ja valentsitsooni seisundite vahel loob eelduse kross-luminestsentsi lainepikkuse nihkumiseks vaakum-ultravioletist ultravioletsesse ja nähtavasse piirkonda, kus seda on tõhusam kaasaegsete kiirete detektoritega registreerida.

Töö käigus süteesiti $BaGeF_6$, K_2GeF_6, K_2SiF_6 ja Na_2GeF_6 heksafluoriidide mikropulbrid. Pulbrite faasipuhtus kontrolliti röntgendifraktsioonanalüüsi abil ning nende morfoloogia selgitati välja skaneeriva elektronmikroskoobi abil. Pulbrite luminestsents- ja optiliste omaduste välja selgitamiseks rakendati erinevaid luminestsentsspektroskoopia meetodeid nii Tartu Ülikooli füüsika instituudi laborites kui ka neljanda põlvkonna sünkrotronkiirguse keskuses MAX IV (Lund, Rootsi) FinEstBeAMS ja FemtoMAX kiirekanalitel. Võtmetähtsusega olid seejuures suure ajalise lahutusega luminestsentsspektroskoopia katsed, mida viidi läbi ülilühikeste elektronkimpude (60 ps) ning sünkrotronkiirguse (< 200 fs) ergastusel. Spetsiaalselt suure ajalise lahutusega eksperimentideks konstrueeriti teisaldatav katseseade, millega saavutati suurepärane 32 ps ajaline lahutusvõime FemtoMAX kiirekanalil.

Läbi viidud katsete tulemusena tuvastati erinevate omakiirguste tekkimise protsessid, milleks olid nii ülikiired alla nanosekundilise kestvusega kross-luminestsents ja tsoonisisese luminestsentsi kiirgused kui ka aeglased mikrosekunditesse ulatuvad iselõksustunud eksitonide kiirgused uuritud materjalides. Ülikiirete, alla 500 ps kustumisajaga kiirguste esinemist näidati laias spektraalses vahemikus vaakum-ultravioletist nähtavani. Katsete tulemuste kombineerimisel arvutuslike andmetega oli võimalik erinevate kiirgusribade seostamine kross-luminestsentsi ja tsoonisisese luminestsentsi kiirguslike üleminekutega baastsooni ja valentsitsooni alamtsoonide vahel. Näidati, et kolmekomponendilistes heksafluoriidides tekkivad ülikiire kustumisajaga kross-luminestsents ja tsoonisisese luminestsentsi kiirgused esinevad kaasaegsete kiirete detektorite jaoks sobilikus, ultravioletse ja nähtava valguse piirkonnas.

Doktoritöö tulemusena näidati, et tsoonistruktuuri modifitseerimise lähenemist saab edukalt rakendada kaasaegsete tipptasemel arvutuslike ja eksperimentaalsete meetodite ühendamiseks, et töötada välja uusi stsintillaatoreid, millel on soovitud spetsiifilised luminestsentsomadused.

9. ACKNOWLEDGEMENTS

I would like to thank my supervisor Prof. Marco Kirm for his guidance and support during my studies.

I would also like to thank Dr. Alexander Vanetsev for synthesizing the samples studied in this work, Dr. Hugo Mändar of performing XRD analysis and Dr. Siim Pikker for carrying out studies by scanning electron microscopy of the samples. I am grateful to Dr. Vitali Nagirnyi, Dr. Eduard Feldbach, Dr. Sergey Omelkov, Dr. Kirill Chernenko (MAX IV, Lund, Sweden), Dr. Ivo Romet and others who helped to carry out different measurements and were involved in data processing in Tartu and Lund. All my fellow colleagues from the Laboratory of Physics of Ionic Crystals in Tartu are appreciated for their support.

I am grateful to my wife and daughter, my parents and friends for their support. I also appreciate the support shown by my colleagues from the Radiology Clinic of Tartu University Hospital.

10. REFERENCES

[1] C. Dujardin, E. Auffray, E. Bourret-Courchesne, P. Dorenbos, P. Lecoq, M. Nikl, A.N. Vasil'ev, A. Yoshikawa, R.-Y. Zhu, Needs, trends, and advances in inorganic scintillators, IEEE Transactions on Nuclear Science 65 (2018) 1977–1997, doi: 10.1109/ TNS.2018.2840160.

[2] P. Lecoq, C. More, J.O. Prior, D. Visvikis, S. Gundacker, E. Auffray, P. Križan, R.M. Turtos, D. Thers, E. Charbon, J. Varela, C. de La Taille, A. Rivetti, D. Breton, J.-F. Pratte, J. Nuyts, S. Surti, S. Vandenberghe, P. Marsden, K. Parodi, J.M. Benlloch, M. Benoit, Roadmap toward the 10 ps time-of-flight PET challenge, Physics in Medicine & Biology 65 (2020) 21RM01, doi: 10.1088/1361-6560/ab9500.

[3] R.H. Pots, E. Auffray, S. Gundacker, Exploiting cross-luminescence in BaF_2 for ultrafast timing applications using deep-ultraviolet sensitive HPK silicon photo-multipliers, Frontiers in Physics 8 (2020) 592875, doi: 10.3389/fphy.2020. 592875.

[4] S. Gundacker, E. Auffray, K. Pauwels, P. Lecoq, Measurement of intrinsic rise times for various L(Y)SO and LuAG scintillators with a general study of prompt photons to achieve 10 ps in TOF-PET, Physics in Medicine & Biology 61 (2016) 2802–2837, doi: 10.1088/0031-9155/61/7/2802.

[5] Y. Shao, A new timing model for calculating the intrinsic timing resolution of a scintillator detector, Physics in Medicine and Biology, 52 (2007) 1103–17, doi: 10.1088/0031-9155/52/4/016.

[6] P. Dorenbos, Fundamental Limitations in the Performance of Ce^{3+}–, Pr^{3+}–, and Eu^{2+}–Activated Scintillators, IEEE Transactions on Nuclear Science, 57 (2010) 1162–1167, doi: 10.1109/TNS.2009.2031140.

[7] A. Vasil'ev, Relaxation of hot electronic excitations in scintillators: Account for scattering, track effects, complicated electronic structure, Proceedings of The Fifth International Conference on Inorganic Scintillators and Their Applications (SCINT) (1999) 43–52.

[8] P. Lecoq, M. Korzhik, A. Vasil'ev, Nuclear science, can transient phenomena help improving time resolution in scintillators? IEEE Trans 61 (2014) 229–234, doi: 10.1109/TNS.2013.2282232.

[9] V.N. Makhov, Vacuum ultraviolet luminescence of wide band-gap solids studied using time-resolved spectroscopy with synchrotron radiation, Physica Scripta 89 (2014) 044010, doi: 10.1088/0031-8949/89/04/044010.

[10] Yu.M. Aleksandrov, V.N. Makhov, P.A. Rodnyi, T.I. Syrejshchikova, M. N. Yaki-menko, Intrinsic luminescence of BaF_2 at pulsed synchrotron radiation excitation, Soviet Physics – Solid State 26 (1984) 2865–2867.

[11] C.W.E. van Eijk, Cross-luminescence, Journal of Luminescence, vol. 60&61 (1994) 936-941, doi: 10.1016/0022-2313(94)90316-6.

[12] M.A. Terekhin, A.N. Vasil'ev, M. Kamada, E. Nakamura, S. Kubota, Effect of quenching processes on the decay of fast luminescence from barium fluoride excited by VUV synchrotron-radiation, Physics Review B 52 (1995) 3117–3121, doi: 10.1103/PhysRevB.52.3117.

[13] P. Dorenbos, R. Visser, J. Andriessen, C.W.E. van Eijk, J. Valbis, N.M. Khaidukov, Scintillation properties of possible cross-luminescence materials, Nuclear Tracks and Radiation Measurements 21 (1993) 101–103, doi: 10.1016/1359-0189(93)90052-B.

[14] S. Gundacker, R.H. Pots, A. Nepomnyashchikh, E. Radzhabov, R. Shendrik, S. Omelkov, M. Kirm, F. Acerbi, M. Capasso, G. Paternoster, A. Mazzi, A. Gola, J. Chen, E. Auffray, Vacuum ultraviolet silicon photomultipliers applied to BaF_2 cross-luminescence detection for high-rate ultrafast timing application, Physics in Medicine & Biology, 66 (2021) 114002, doi: 10.1088/1361-6560/abf476.

[15] V.N. Makhov, I. Kuusmann, J. Becker, M. Runne, G. Zimmerer, Crossluminescence at high temperatures, Journal of Electron Spectroscopy and Related Phenomena, 101 (1999) 817–820, doi: 10.1016/S0368-2048(98)00430-7.

[16] M.G. Brik, A. Srivastava, Ab initio studies of the structural, electronic, and optical properties of K_2SiF_6 single crystals at ambient and elevated hydrostatic pressure, Journal of the Electrochemical Society 159 (2012) J212–J216, doi: 10.1149/2.071206jes.

[17] V. Vaněček, J. Páterek, R. Král, R. Kučerková, V. Babin, J. Rohlíček, R. Cala', N. Kratochwil, E. Auffray, M. Nikl, Ultraviolet cross-luminescence in ternary chlorides of alkali and alkaline-earth metals, Optical Materials: X 12 (2021) 100103, doi: 10.1016/j.omx.2021.100103.

[18] D.I. Vaisburd, V.T. Shkatov, E.G. Tavanov, B.N. Semin, S.G. Akerman, Nano-second relaxation of conductivity and luminescence spectra of ionic crystals during super-dense excitation by power electron-beam, Izv. Nauk AS USSR. Phys. Ser. 38, (1974) 1281–1284.

[19] D. Vaisburd, S. Kharitonova, Two types of fundamental luminescence of ionization-passive electrons and holes in optical dielectrics – intraband-electron and interband-hole luminescence (theoretical calculation and comparison with experiment), Russian Physics Journal 40 (11) (1997) 1037–1060, doi: 10.1007/BF02508940.

[20] R. G. Deich, M. S. Abdrakhmanov, Intraband luminescence in ionic crystals, physica status solidi (b) 171 (1992) 263–273, doi: 10.1002/pssb.2221710129.

[21] S.I. Omelkov, V. Nagirnyi, M. Kirm, M. Korzik, A. Gektin (Eds.), New Properties and Prospects of Hot Intraband Luminescence for Fast Timing, Springer Proceedings in Physics, 227 (2019) 41–53, doi: 10.1007/978-3-030-21970-3.

[22] S.I. Omelkov, V. Nagirnyi, S. Gundacker, D.A. Spassky, E. Auffray, P. Lecoq, M. Kirm, Scintillation yield of hot intraband luminescence, Journal of Luminescence, 198 (2018) 260–271, doi: 10.1016/j.jlumin.2018.02.027.

[23] R. M. Turtos, S. Gundacker, S. Omelkov, B. Mahler, A. H. Khan, J. Saaring, Z. Meng, A. Vasil'ev, C. Dujardin, M. Kirm, I. Moreels, E. Auffray, P. Lecoq, On the use of CdSe scintillating nanoplatelets as time taggers for high-energy gamma detection, npj 2D Materials and Applications 3 (2019) 37, doi: 10.1038/s41699-019-0120-8.

[24] S. Gundacker, R.M. Turtos, N. Kratochwil, R. H. Pots, M. Paganoni, P. Lecoq, E. Auffray, Experimental time resolution limits of modern SiPMs and TOF-PET detectors exploring different scintillators and Cherenkov emission, Physics in Medicine & Biology, 65 (2020) 025001, doi: 10.1088/1361-6560/ab63b4.

[25] G. Gallina, P. Giampa, F. Retière et al., Characterization of the Hamamatsu VUV4 MPPCs for nEXO, Nuclear Instruments and Methods in Physics Research, Section A 940 (2019) 371–379, doi: 10.1016/j.nima.2019.05.096.

[26] A. Vanetsev, P. Põdder, M. Oja, N.M. Khaidukov, V.N. Makhov, V. Nagirnyi, I. Romet, S. Vielhauer, H. Mändar, M. Kirm, Microwave-hydrothermal synthesis and investigation of Mn-doped K_2SiF_6 microsize powder as a red phosphor for warm white LEDs, Journal of Luminescence 239 (2021) 118389, doi: 10.1016/j.jlumin.2021.118389.

[27] E. Feldbach, E. Tõldsepp, M. Kirm, A. Lushchik, K. Mizohata, J. Räisänen, Radiation resistance diagnostics of optical materials, Opt. Mater. 55 (2016) 164–167, doi: 10.1016/j.optmat.2016.03.008.

[28] S.I. Omelkov, V. Nagirnyi, A.N. Vasil'ev, M. Kirm, New features of hot intraband luminescence for fast timing, Journal of Luminescence, 176 (2016) 309–317, doi: 10.1016/j.jlumin.2016.03.039.

[29] S.I. Omelkov, V. Nagirnyi, S. Gundacker, D.A. Spassky, E. Auffray, P. Lecoq, M. Kirm, Scintillation yield of hot intraband luminescence, J. Lumin. 198 (2018) 260–271, doi: 10.1016/j.jlumin.2018.02.027.

[30] R. Pärna, R. Sankari, E. Kukk, E. Nõmmiste, M. Valden, M. Lastusaari, K. Kooser, K. Kokko, M. Hirsimäki, S. Urpelainen, P. Turunen, A. Kivimäki, V. Pankratov, L. Reisberg, F. Hennies, H. Tarawneh, R. Nyholm, M. Huttula, FinEstBeaMS — a wide-range Finnish-Estonian beamline for materials science at the 1.5 GeV storage ring at the MAX IV laboratory, Nucl. Instrum. Methods Phys. Res. A 859 (2017) 83–89, doi: 10.1016/j.nima.2017.04.002.

[31] V. Pankratov, R. Pärna, M. Kirm, V. Nagirnyi, E. Nõmmiste, S. Omelkov, S. Vielhauer, K. Chernenko, L. Reisberg, P. Turunen, A. Kivimäki, E. Kukk, M. Valden, M. Huttula, Progress in development of a new luminescence setup at the FinEstBeAMS beamline of the MAX IV laboratory, Radiation Measurements 121 (2019) 91–98, doi: 10.1016/j.radmeas.2018.12.011.

[32] K. Chernenko, A. Kivimäki, R. Pärna, W. Wang, R. Sankari, M. Leandersson, H. Tarawneh, V. Pankratov, M. Kook, E. Kukk, L. Reisberg, S. Urpelainen, T. Käämbre, F. Siewert, G. Gwalt, A. Sokolov, S. Lemke, S. Alimov, J. Knedel, O. Kutz, T. Seliger, M. Valden, M. Hirsimäki, M. Kirm, M. Huttula, Performance and characterization of the FinEstBeAMS beamline at the MAX IV laboratory, Journal of Synchrotron Radiation 28 (2021) 5, doi: 10.1107/ S1600577521006032.

[33] J. Saaring, A. Vanetsev, K. Chernenko, E. Feldbach, I. Kudryavtseva, H. Mändar, R. Pärna, V. Nagirnyi, S. Omelkov, I. Romet, O. Rebane, M. Kirm, Relaxation of electronic excitations in K_2GeF_6 studied by means of time-resolved luminescence spectroscopy under VUV and pulsed electron beam excitation, Journal of Alloys and Compounds, 883 (2021) 160916, https://doi.org/10.1016/j.jallcom.2021.160916.

[34] H. Enquist, A. Jurgilaitis, A. Jarnac, Å.U.J. Bengtsson, M. Burza, F. Curbis, C. Disch, J.C. Ekström, M. Harb, L. Isaksson, M. Kotur, D. Kroon, F. Lindau, E. Mansten, J. Nygaard, A.I.H. Persson, V.T. Pham, M. Rissi, S. Thorin, C.-M. Tu, E. Wallén, X. Wang, S. Werin, J. Larsson, FemtoMAX – an X-ray beamline for structural dynamics at the short-pulse facility of MAX IV, Journal of Synchrotron Radiation, 25 (2018) 570–579, doi: 10.1107/S1600577517017660.

[35] S.I. Omelkov, K. Chernenko, J.C. Ekström, A. Jurgilaitis, A. Khadiev, A. Kivimäki, A. Kotlov, D. Kroon, J. Larsson, V. Nagirnyi, D.V. Novikov, V.-T. Pham, R. Pärna, I. Romet, J. Saaring, I. Schostak, E. Tiirinen, A. Tõnisoo, M. Kirm, Recent advances in time-resolved luminescence spectroscopy at MAX IV and PETRA III storage rings, Journal of Physics: Conference Series. Proceedings of the 14th International Conference on Synchrotron Radiation Instrumentation (2022) in press.

[36] P. Dorenbos, R. Visser, R. Dool, J. Andriessen, C.W.E. van Eijk, Suppression of self-trapped exciton luminescence in La^{3+}- and Nd^{3+}-doped BaF_2, Journal of Physics: Condensed Matter 4 (1992) 5281, doi: 10.1088/0953-8984/4/23/005.

[37] M. Kirm, A. Lushchik, Ch. Lushchik, A.I. Nepomnyashikh, F. Savikhin, Dependence of the efficiency of various emissions on excitation density in BaF_2 crystals, Radiation Measurements 33 (2001) 515–519, doi: 10.1016/S1350-4487(01) 00044-0.

[38] M. Kirm, V. Nagirnyi, S. Vielhauer, E. Feldbach, Relaxation and interaction of electronic excitations induced by intense ultrashort light pulses in BaF_2 scintillator, L. Juha, S. Bajt, R. Sobierajski, (Eds.), Damage to VUV, EUV, and X-Ray Optics II. SPIE Proceedings 8077 (2011) 8077-U1-U8, doi: 10.1117/12.887601.

[39] O. Isayev, C. Oses, C. Toher, E. Gossett, S. Curtarolo, A. Trophsa, Universal fragment descriptors for predicting properties of inorganic crystals, Nature Communications 8 (2017) 15679, doi: 10.1038/ncomms15679.

[40] J. Saaring, A. Vanetsev, K. Chernenko, E. Feldbach, I. Kudryavtseva, H. Mändar, S. Pikker, R. Pärna, V. Nagirnyi, S. Omelkov, I. Romet, O. Rebane, M. Kirm, Time-resolved luminescence spectroscopy of ultrafast emissions in $BaGeF_6$, Journal of Luminescence 244 (2022) 118729, doi: 10.1016/j.jlumin.2022.118729.

[41] K.S. Song, R.T. Williams, Self-Trapped Excitons, vol. 105 (1993) Springer, Berlin, doi: 10.1007/978-3-642-85236-7.

[42] K. Persson, Materials Data on K_2GeF_6 (SG:164) by Materials Project, doi: 10.17188/1307631.

11. PUBLICATIONS

CURRICULUM VITAE

Name: Juhan Saaring
Date of birth: 24.05.1990
Citizenship: Estonian
Address: Institute of Physics, University of Tartu, W. Ostwald Str. 1, 50411, Estonia
E-mail: juhan.saaring@ut.ee

Current positions: Laboratory of Physics of Ionic Crystals, Institute of Physics, University of Tartu, Spectroscopy Specialist
Radiology Clinic, Tartu University Hospital, Medical Physicist

Education:

2013–2015 Tallinn University of Technology and University of Tartu, MSc in Medical Physics, *cum laude*
2010–2013 Tallinn University of Technology, BSc in Engineering Physics
2006–2009 Nõo Science High School

Language skills: Estonian (mother tongue), English (very good),

Institution and position held:

2020– University of Tartu, Faculty of Science and Technology, Institute of Physics, Laboratory of Physics of Ionic Crystals, Spectroscopy Specialist
2015– Radiology Clinic, Tartu University Hospital, Medical Physicist

Research interests:

Ultrafast relaxation processes in scintillators to be used in a wide range of applications that require high time resolution.

Publications:

J. Saaring, E. Feldbach, V. Nagirnyi, S. Omelkov, A. Vanetsev, M. Kirm, Ultrafast radiative relaxation processes in multication cross-luminescence materials, IEEE Trans. on Nucl. Science **67** (2020) 1009–1013, https://doi.org/10.1109/TNS.2020.2974071.

J. Saaring, A. Vanetsev, K. Chernenko, E. Feldbach, I. Kudryavtseva, H. Mändar, R. Pärna, V. Nagirnyi, S. Omelkov, I. Romet, O. Rebane, M. Kirm, Relaxation of electronic excitations in K_2GeF_6 studied by means of time-resolved luminescence spectroscopy under VUV and pulsed electron beam excitation, Journal of Alloys and Compounds **883** (2021) 160916, https://doi.org/10.1016/j.jallcom.2021.160916.

J. Saaring, A. Vanetsev, K. Chernenko, E. Feldbach, I. Kudryavtseva, H. Mändar, S. Pikker, R. Pärna, V. Nagirnyi, S. Omelkov, I. Romet, O. Rebane, M. Kirm, Time-resolved luminescence spectroscopy of ultrafast emissions in $BaGeF_6$, Journal of Luminescence **244** (2022) 118729, https://doi.org/10.1016/j.jlumin.2022.118729.

S.I. Omelkov, K. Chernenko, J.C. Ekström, A. Jurgilaitis, A. Khadiev, A. Kivi-mäki, A. Kotlov, D. Kroon, J. Larsson, V. Nagirnyi, D.V. Novikov, V.-T. Pham, R. Pärna, I. Romet, **J. Saaring**, I. Schostak, E. Tiirinen, A. Tõnisoo, M. Kirm, Recent advances in time-resolved luminescence spectroscopy at MAX IV and PETRA III storage rings, Journal of Physics: Conference Series. Proceedings of the 14th International Conference on Synchrotron Radiation Instrumentation (2022) in press.

R. M. Turtos, S. Gundacker, S. Omelkov, B. Mahler, A. H. Khan, **J. Saaring**, Z. Meng, A. Vasil'ev, C. Dujardin, M. Kirm, I. Moreels, E. Auffray, P. Lecoq, On the use of CdSe scintillating nanoplatelets as time taggers for high-energy gamma detection, npj 2D Materials and Applications **3** (2019) 37, https://doi.org/10.1038/s41699-019-0120-8.

Conference presentations:

J. Saaring, S. Omelkov, E. Feldbach, V. Nagirnyi, I. Romet, A. Vanetsev, M. Kirm, "Relaxation of anion and cation electronic excitations in hexafluorogermanates", oral presentation at the 11th International Conference on Luminescent Detectors and Transformers of Ionizing Radiation, 2021, Bydgoszcz, Poland.

J. Saaring, S. Omelkov, E. Feldbach, V. Nagirnyi, I. Romet, A. Vanetsev, M. Kirm, "Anion and cation excitations in hexafluorogermanates", oral presentation at the Graduate School of Functional Materials and Technologies Scientific Conference, 2021, Tartu, Estonia.

J. Saaring, E. Feldbach, I. Kudryavtseva, V. Nagirnyi, S. Omelkov, I. Romet, S. Roy, A. Vanetsev, M. Kirm, "Ultrafast Cross-Luminescence in $BaGeF_6$ and K_2GeF_6" oral presentation at the International Conference Functional Materials and Nanotechnologies, 2020, Vilnius, Lithuania (presented online).

J. Saaring, E. Feldbach, V. Nagirnyi, S. Omelkov, I. Romet, A. Vanetsev, M. Kirm, "Ultrafast Cross-Luminescence in Germanium-based Fluorides", poster presentation at the Graduate School of Functional Materials and Technologies Scientific Conference, 2020, Tallinn, Estonia.

J. Saaring, E. Feldbach, V. Nagirnyi, S. Omelkov, A. Vanetsev, M. Kirm, "Ultrafast Radiative Relaxation Processes in Multication Cross-Luminescence Materials", oral presentation at the International Conference on Scintillating Materials and their Applications, 2019, Sendai, Japan.

J. Saaring, M. Kirm, S. Omelkov, E. Feldbach, V. Nagirnyi, E.D. Bourret, I. Romet, P. Lecoq, "LaOF Luminescence Spectroscopy", poster presentation at the Graduate School of Functional Materials and Technologies Scientific Conference, 2019, Tartu, Estonia.

Awards and scholarships:

2013, 2014 University of Tartu Foundation, Ole Golubjatnikov Memorial Scholarship

Courses attended:

LUMDETR 2021 Summer School on scintillation, dosimetric and phosphor materials, 10–11 September 2021, Bydgoszcz, Poland.

SCINT 2019 Summer School on crystal growing techniques, 26–28 September 2019, Sendai, Japan.

ELULOOKIRJELDUS

Nimi: Juhan Saaring
Sünniaeg: 24.05.1990
Kodakondsus: Eesti
Aadress: Füüsika Instituut, Tartu Ülikool, W. Ostwaldi tn 1, 50411, Tartu
E-post: juhan.saaring@ut.ee

Praegune töökoht: Ioonkristallide füüsika labor, Füüsika Insituut, Tartu Ülikool, spektroskoopia spetsialist
Radioloogiakliinik, Tartu Ülikooli Kliinikum, meditsiinifüüsik

Haridus:

2013–2015   Tallinna Tehnikaülikool ja Tartu Ülikool, MSc biomeditsiinitehnoloogia ja meditsiinifüüsika, *cum laude*
2010–2013   Tallinna Tehnikaülikool, BSc tehniline füüsika
2006–2009   Nõo Reaalgümnaasium

Keelteoskus: eesti (emakeel), inglise (väga hea)

Töökogemus:

2020–   Ioonkristallide füüsika labor, Füüsika Insituut, Tartu Ülikool, spektroskoopia spetsialist
2015–   Radioloogiakliinik, Tartu Ülikooli Kliinikum, meditsiinifüüsik

Peamised uurimisvaldkonnad:

Ülikiired relaksatsiooniprotsesside uurimine stsintillaatorites eesmärgiga leida uusi materjale, mille ajaline lahutusvõime vastaks tänapäeva aplikatsioonide kõrgetele nõudmistele

Publikatsioonid:

J. Saaring, E. Feldbach, V. Nagirnyi, S. Omelkov, A. Vanetsev, M. Kirm, Ultrafast radiative relaxation processes in multication cross-luminescence materials, IEEE Trans. on Nucl. Science **67** (2020) 1009–1013, https://doi.org/10.1109/TNS.2020.2974071.

J. Saaring, A. Vanetsev, K. Chernenko, E. Feldbach, I. Kudryavtseva, H. Mändar, R. Pärna, V. Nagirnyi, S. Omelkov, I. Romet, O. Rebane, M. Kirm, Relaxation of electronic excitations in K2GeF6 studied by means of time-resolved luminescence spectroscopy under VUV and pulsed electron beam excitation, Journal of Alloys and Compounds **883** (2021) 160916, https://doi.org/10.1016/j.jallcom.2021.160916.

J. Saaring, A. Vanetsev, K. Chernenko, E. Feldbach, I. Kudryavtseva, H. Mändar, S. Pikker, R. Pärna, V. Nagirnyi, S. Omelkov, I. Romet, O. Rebane, M. Kirm, Time-resolved luminescence spectroscopy of ultrafast emissions in $BaGeF_6$, Journal of Luminescence **244** (2022) 118729, https://doi.org/10.1016/j.jlumin.2022.118729.

S.I. Omelkov, K. Chernenko, J.C. Ekström, A. Jurgilaitis, A. Khadiev, A. Kivimäki, A. Kotlov, D. Kroon, J. Larsson, V. Nagirnyi, D.V. Novikov, V.-T. Pham, R. Pärna, I. Romet, **J. Saaring**, I. Schostak, E. Tiirinen, A. Tõnisoo, M. Kirm, Recent advances in time-resolved luminescence spectroscopy at MAX IV and PETRA III storage rings, Journal of Physics: Conference Series. Proceedings of the 14th International Conference on Synchrotron Radiation Instrumentation (2022) trükis.

R. M. Turtos, S. Gundacker, S. Omelkov, B. Mahler, A. H. Khan, **J. Saaring**, Z. Meng, A. Vasil'ev, C. Dujardin, M. Kirm, I. Moreels, E. Auffray, P. Lecoq, On the use of CdSe scintillating nanoplatelets as time taggers for high-energy gamma detection, npj 2D Materials and Applications **3** (2019) 37, https://doi.org/10.1038/s41699-019-0120-8.

Konverentsiettekanded:

J. Saaring, S. Omelkov, E. Feldbach, V. Nagirnyi, I. Romet, A. Vanetsev, M. Kirm, "Relaxation of anion and cation electronic excitations in hexafluorogermanates", suuline ettekanne rahvusvahelisel konverentsil Luminescent Detectors and Transformers of Ionizing Radiation, 2021, Bydgoszcz, Poola.

J. Saaring, S. Omelkov, E. Feldbach, V. Nagirnyi, I. Romet, A. Vanetsev, M. Kirm, "Anion and cation excitations in hexafluorogermanates", suuline ettekanne funktsionaalsete materjalide ja tehnoloogiate doktorikooli teaduskonverentsil, 2021, Tartu, Estonia.

J. Saaring, E. Feldbach, I. Kudryavtseva, V. Nagirnyi, S. Omelkov, I. Romet, S. Roy, A. Vanetsev, M. Kirm, "Ultrafast Cross-Luminescence in $BaGeF_6$ and K_2GeF_6", suuline ettekanne rahvusvahelisel konverentsil Functional Materials and Nanotechnologies, 2020, Vilnius, Leedu (veebi vahendusel).

J. Saaring, E. Feldbach, V. Nagirnyi, S. Omelkov, I. Romet, A. Vanetsev, M. Kirm, "Ultrafast Cross-Luminescence in Germanium-based Fluorides", stendiettekanne funktsionaalsete materjalide ja tehnoloogiate doktorikooli teaduskonverentsil, 2020, Tallinn, Eesti.

J. Saaring, E. Feldbach, V. Nagirnyi, S. Omelkov, A. Vanetsev, M. Kirm, "Ultrafast Radiative Relaxation Processes in Multication Cross-Luminescence Materials", suuline ettekanne rahvusvahelisel konverentsil Scintillating Materials and their Applications, 2019, Sendai, Jaapan.

J. Saaring, M. Kirm, S. Omelkov, E. Feldbach, V. Nagirnyi, E.D. Bourret, I. Romet, P. Lecoq, "LaOF Luminescence Spectroscopy", stendiettekanne Funktsionaalsete materjalide ja tehnoloogiate doktorikooli teaduskonverentsil, 2019, Tartu, Eesti.

Saadud uurimistoetused ja stipendiumid:

2013, 2014 Tartu Ülikooli sihtasutus, Ole Golubjatnikovi mälestusstipendium

Osalemine kursustel:

LUMDETR 2021 suvekool stsintillaatoritest, dosimeetrilistest ja fosfoor-materjalidest, 10.–11. september 2021, Bydgoszcz, Poola.

SCINT 2019 suvekool kristallide kasvatamise tehnoloogiatest, 26.–28. september 2019, Sendai, Jaapan.

DISSERTATIONES PHYSICAE
UNIVERSITATIS TARTUENSIS

1. **Andrus Ausmees.** XUV-induced electron emission and electron-phonon interaction in alkali halides. Tartu, 1991.
2. **Heiki Sõnajalg.** Shaping and recalling of light pulses by optical elements based on spectral hole burning. Tartu, 1991.
3. **Sergei Savihhin.** Ultrafast dynamics of F-centers and bound excitons from picosecond spectroscopy data. Tartu, 1991.
4. **Ergo Nõmmiste.** Leelishalogeniidide röntgenelektronemissioon kiiritamisel footonitega energiaga 70–140 eV. Tartu, 1991.
5. **Margus Rätsep.** Spectral gratings and their relaxation in some low-temperature impurity-doped glasses and crystals. Tartu, 1991.
6. **Tõnu Pullerits.** Primary energy transfer in photosynthesis. Model calculations. Tartu, 1991.
7. **Olev Saks.** Attoampri diapasoonis voolude mõõtmise füüsikalised alused. Tartu, 1991.
8. **Andres Virro.** AlGaAsSb/GaSb heterostructure injection lasers. Tartu, 1991.
9. **Hans Korge.** Investigation of negative point discharge in pure nitrogen at atmospheric pressure. Tartu, 1992.
10. **Jüri Maksimov.** Nonlinear generation of laser VUV radiation for high-resolution spectroscopy. Tartu, 1992.
11. **Mark Aizengendler.** Photostimulated transformation of aggregate defects and spectral hole burning in a neutron-irradiated sapphire. Tartu, 1992.
12. **Hele Siimon.** Atomic layer molecular beam epitaxy of A^2B^6 compounds described on the basis of kinetic equations model. Tartu, 1992.
13. **Tõnu Reinot.** The kinetics of polariton luminescence, energy transfer and relaxation in anthracene. Tartu, 1992.
14. **Toomas Rõõm.** Paramagnetic H^{2-} and F^+ centers in CaO crystals: spectra, relaxation and recombination luminescence. Tallinn, 1993.
15. **Erko Jalviste.** Laser spectroscopy of some jet-cooled organic molecules. Tartu, 1993.
16. **Alvo Aabloo.** Studies of crystalline celluloses using potential energy calculations. Tartu, 1994.
17. **Peeter Paris.** Initiation of corona pulses. Tartu, 1994.
18. **Павел Рубин.** Локальные дефектные состояния в CuO_2 плоскостях высокотемпературных сверхпроводников. Тарту, 1994.
19. **Olavi Ollikainen.** Applications of persistent spectral hole burning in ultra-fast optical neural networks, time-resolved spectroscopy and holographic interferometry. Tartu, 1996.
20. **Ülo Mets.** Methodological aspects of fluorescence correlation spectroscopy. Tartu, 1996.
21. **Mikhail Danilkin.** Interaction of intrinsic and impurity defects in CaS:Eu luminophors. Tartu, 1997.

22. **Ирина Кудрявцева.** Создание и стабилизация дефектов в кристаллах KBr, KCl, RbCl при облучении ВУФ-радиацией. Тарту, 1997.

23. **Andres Osvet.** Photochromic properties of radiation-induced defects in diamond. Tartu, 1998.

24. **Jüri Örd.** Classical and quantum aspects of geodesic multiplication. Tartu, 1998.

25. **Priit Sarv.** High resolution solid-state NMR studies of zeolites. Tartu, 1998.

26. **Сергей Долгов.** Электронные возбуждения и дефектообразование в некоторых оксидах металлов. Тарту, 1998.

27. **Kaupo Kukli.** Atomic layer deposition of artificially structured dielectric materials. Tartu, 1999.

28. **Ivo Heinmaa.** Nuclear resonance studies of local structure in $RBa_2Cu_3O_{6+x}$ compounds. Tartu, 1999.

29. **Aleksander Shelkan.** Hole states in CuO_2 planes of high temperature superconducting materials. Tartu, 1999.

30. **Dmitri Nevedrov.** Nonlinear effects in quantum lattices. Tartu, 1999.

31. **Rein Ruus.** Collapse of 3d (4f) orbitals in 2p (3d) excited configurations and its effect on the x-ray and electron spectra. Tartu, 1999.

32. **Valter Zazubovich.** Local relaxation in incommensurate and glassy solids studied by Spectral Hole Burning. Tartu, 1999.

33. **Indrek Reimand.** Picosecond dynamics of optical excitations in GaAs and other excitonic systems. Tartu, 2000.

34. **Vladimir Babin.** Spectroscopy of exciton states in some halide macro- and nanocrystals. Tartu, 2001.

35. **Toomas Plank.** Positive corona at combined DC and AC voltage. Tartu, 2001.

36. **Kristjan Leiger.** Pressure-induced effects in inhomogeneous spectra of doped solids. Tartu, 2002.

37. **Helle Kaasik.** Nonperturbative theory of multiphonon vibrational relaxation and nonradiative transitions. Tartu, 2002.

38. **Tõnu Laas.** Propagation of waves in curved spacetimes. Tartu, 2002.

39. **Rünno Lõhmus.** Application of novel hybrid methods in SPM studies of nanostructural materials. Tartu, 2002.

40. **Kaido Reivelt.** Optical implementation of propagation-invariant pulsed free-space wave fields. Tartu, 2003.

41. **Heiki Kasemägi.** The effect of nanoparticle additives on lithium-ion mobility in a polymer electrolyte. Tartu, 2003.

42. **Villu Repän.** Low current mode of negative corona. Tartu, 2004.

43. **Алексей Котлов.** Оксианионные диэлектрические кристаллы: зонная структура и электронные возбуждения. Tartu, 2004.

44. **Jaak Talts.** Continuous non-invasive blood pressure measurement: comparative and methodological studies of the differential servo-oscillometric method. Tartu, 2004.

45. **Margus Saal.** Studies of pre-big bang and braneworld cosmology. Tartu, 2004.

46. **Eduard Gerškevitš.** Dose to bone marrow and leukaemia risk in external beam radiotherapy of prostate cancer. Tartu, 2005.
47. **Sergey Shchemelyov.** Sum-frequency generation and multiphoton ionization in xenon under excitation by conical laser beams. Tartu, 2006.
48. **Valter Kiisk.** Optical investigation of metal-oxide thin films. Tartu, 2006.
49. **Jaan Aarik.** Atomic layer deposition of titanium, zirconium and hafnium dioxides: growth mechanisms and properties of thin films. Tartu, 2007.
50. **Astrid Rekker.** Colored-noise-controlled anomalous transport and phase transitions in complex systems. Tartu, 2007.
51. **Andres Punning.** Electromechanical characterization of ionic polymer-metal composite sensing actuators. Tartu, 2007.
52. **Indrek Jõgi.** Conduction mechanisms in thin atomic layer deposited films containing TiO_2. Tartu, 2007.
53. **Aleksei Krasnikov.** Luminescence and defects creation processes in lead tungstate crystals. Tartu, 2007.
54. **Küllike Rägo.** Superconducting properties of MgB_2 in a scenario with intra- and interband pairing channels. Tartu, 2008.
55. **Els Heinsalu.** Normal and anomalously slow diffusion under external fields. Tartu, 2008.
56. **Kuno Kooser.** Soft x-ray induced radiative and nonradiative core-hole decay processes in thin films and solids. Tartu, 2008.
57. **Vadim Boltrushko.** Theory of vibronic transitions with strong nonlinear vibronic interaction in solids. Tartu, 2008.
58. **Andi Hektor.** Neutrino Physics beyond the Standard Model. Tartu, 2008.
59. **Raavo Josepson.** Photoinduced field-assisted electron emission into gases. Tartu, 2008.
60. **Martti Pärs.** Study of spontaneous and photoinduced processes in molecular solids using high-resolution optical spectroscopy. Tartu, 2008.
61. **Kristjan Kannike.** Implications of neutrino masses. Tartu, 2008.
62. **Vigen Issahhanjan.** Hole and interstitial centres in radiation-resistant MgO single crystals. Tartu, 2008.
63. **Veera Krasnenko.** Computational modeling of fluorescent proteins. Tartu, 2008.
64. **Mait Müntel.** Detection of doubly charged higgs boson in the CMS detector. Tartu, 2008.
65. **Kalle Kepler.** Optimisation of patient doses and image quality in diagnostic radiology. Tartu, 2009.
66. **Jüri Raud.** Study of negative glow and positive column regions of capillary HF discharge. Tartu, 2009.
67. **Sven Lange.** Spectroscopic and phase-stabilisation properties of pure and rare-earth ions activated ZrO_2 and HfO_2. Tartu, 2010.
68. **Aarne Kasikov.** Optical characterization of inhomogeneous thin films. Tartu, 2010.
69. **Heli Valtna-Lukner.** Superluminally propagating localized optical pulses. Tartu, 2010.

70. **Artjom Vargunin.** Stochastic and deterministic features of ordering in the systems with a phase transition. Tartu, 2010.
71. **Hannes Liivat.** Probing new physics in e+e− annihilations into heavy particles via spin orientation effects. Tartu, 2010.
72. **Tanel Mullari.** On the second order relativistic deviation equation and its applications. Tartu, 2010.
73. **Aleksandr Lissovski.** Pulsed high-pressure discharge in argon: spectroscopic diagnostics, modeling and development. Tartu, 2010.
74. **Aile Tamm.** Atomic layer deposition of high-permittivity insulators from cyclopentadienyl-based precursors. Tartu, 2010.
75. **Janek Uin.** Electrical separation for generating standard aerosols in a wide particle size range. Tartu, 2011.
76. **Svetlana Ganina.** Hajusandmetega ülesanded kui üks võimalus füüsika-õppe efektiivsuse tõstmiseks. Tartu, 2011
77. **Joel Kuusk.** Measurement of top-of-canopy spectral reflectance of forests for developing vegetation radiative transfer models. Tartu, 2011.
78. **Raul Rammula**. Atomic layer deposition of HfO_2 – nucleation, growth and structure development of thin films. Tartu, 2011.
79. **Сергей Наконечный.** Исследование электронно-дырочных и интерстициал-вакансионных процессов в монокристаллах MgO и LiF методами термоактивационной спектроскопии. Тарту, 2011.
80. **Niina Voropajeva.** Elementary excitations near the boundary of a strongly correlated crystal. Tartu, 2011.
81. **Martin Timusk.** Development and characterization of hybrid electro-optical materials. Tartu, 2012, 106 p.
82. **Merle Lust.** Assessment of dose components to Estonian population. Tartu, 2012, 84 p.
83. **Karl Kruusamäe.** Deformation-dependent electrode impedance of ionic electromechanically active polymers. Tartu, 2012, 128 p.
84. **Liis Rebane.** Measurement of the $W \to \tau\nu$ cross section and a search for a doubly charged Higgs boson decaying to τ-leptons with the CMS detector. Tartu, 2012, 156 p.
85. **Jevgeni Šablonin.** Processes of structural defect creation in pure and doped MgO and NaCl single crystals under condition of low or super high density of electronic excitations. Tartu, 2013, 145 p.
86. **Riho Vendt**. Combined method for establishment and dissemination of the international temperature scale. Tartu, 2013, 108 p.
87. **Peeter Piksarv.** Spatiotemporal characterization of diffractive and non-diffractive light pulses. Tartu, 2013, 156 p.
88. **Anna Šugai.** Creation of structural defects under superhigh-dense irradiation of wide-gap metal oxides. Tartu, 2013, 108 p.
89. **Ivar Kuusik.** Soft X-ray spectroscopy of insulators. Tartu, 2013, 113 p.
90. **Viktor Vabson**. Measurement uncertainty in Estonian Standard Laboratory for Mass. Tartu, 2013, 134 p.

91. **Kaupo Voormansik.** X-band synthetic aperture radar applications for environmental monitoring. Tartu, 2014, 117 p.

92. **Deivid Pugal.** hp-FEM model of IPMC deformation. Tartu, 2014, 143 p.

93. **Siim Pikker.** Modification in the emission and spectral shape of photo-stable fluorophores by nanometallic structures. Tartu, 2014, 98 p.

94. **Mihkel Pajusalu**. Localized Photosynthetic Excitons. Tartu, 2014, 183 p.

95. **Taavi Vaikjärv.** Consideration of non-adiabaticity of the Pseudo-Jahn-Teller effect: contribution of phonons. Tartu, 2014, 129 p.

96. **Martin Vilbaste.** Uncertainty sources and analysis methods in realizing SI units of air humidity in Estonia. Tartu, 2014, 111 p.

97. **Mihkel Rähn.** Experimental nanophotonics: single-photon sources- and nanofiber-related studies. Tartu, 2015, 107 p.

98. **Raul Laasner.** Excited state dynamics under high excitation densities in tungstates. Tartu, 2015, 125 p.

99. **Andris Slavinskis.** EST Cube-1 attitude determination. Tartu, 2015, 104 p.

100. **Karlis Zalite**. Radar Remote Sensing for Monitoring Forest Floods and Agricultural Grasslands. Tartu, 2016, 124 p.

101. **Kaarel Piip.** Development of LIBS for *in-situ* study of ITER relevant materials. Tartu, 2016, 93 p.

102. **Kadri Isakar.** ^{210}Pb in Estonian air: long term study of activity concentrations and origin of radioactive lead. Tartu, 2016, 107 p.

103. **Artur Tamm.** High entropy alloys: study of structural properties and irradiation response. Tartu, 2016, 115 p.

104. **Rasmus Talviste.** Atmospheric-pressure He plasma jet: effect of dielectric tube diameter. Tartu, 2016, 107 p.

105. **Andres Tiko.** Measurement of single top quark properties with the CMS detector. Tartu, 2016, 161 p.

106. **Aire Olesk.** Hemiboreal Forest Mapping with Interferometric Synthetic Aperture Radar. Tartu, 2016, 121 p.

107. **Fred Valk.** Nitrogen emission spectrum as a measure of electric field strength in low-temperature gas discharges. Tartu, 2016, 149 p.

108. **Manoop Chenchiliyan.** Nano-structural Constraints for the Picosecond Excitation Energy Migration and Trapping in Photosynthetic Membranes of Bacteria. Tartu, 2016, 115p.

109. **Lauri Kaldamäe.** Fermion mass and spin polarisation effects in top quark pair production and the decay of the higgs boson. Tartu, 2017, 104 p.

110. **Marek Oja.** Investigation of nano-size α- and transition alumina by means of VUV and cathodoluminescence spectroscopy. Tartu, 2017, 89 p.

111. **Viktoriia Levushkina.** Energy transfer processes in the solid solutions of complex oxides. Tartu, 2017, 101 p.

112. **Mikk Antsov.** Tribomechanical properties of individual 1D nanostructures: experimental measurements supported by finite element method simulations. Tartu, 2017, 101 p.

113. **Hardi Veermäe.** Dark matter with long range vector-mediated interactions. Tartu, 2017, 137 p.

114. **Aris Auzans.** Development of computational model for nuclear energy systems analysis: natural resources optimisation and radiological impact minimization. Tartu, 2018, 138 p.

115. **Aleksandr Gurev**. Coherent fluctuating nephelometry application in laboratory practice. Tartu, 2018, 150 p.

116. **Ardi Loot**. Enhanced spontaneous parametric downconversion in plasmonic and dielectric structures. Tartu, 2018, 164 p.

117. **Andreas Valdmann.** Generation and characterization of accelerating light pulses. Tartu, 2019, 85 p.

118. **Mikk Vahtrus.** Structure-dependent mechanical properties of individual one-dimensional metal-oxide nanostructures. Tartu, 2019, 110 p.

119. **Ott Vilson.** Transformation properties and invariants in scalar-tensor theories of gravity. Tartu, 2019, 183 p.

120. **Indrek Sünter.** Design and characterisation of subsystems and software for ESTCube-1 nanosatellite. Tartu, 2019, 195 p.

121. **Marko Eltermann**. Analysis of samarium doped TiO_2 optical and multi-response oxygen sensing capabilities. Tartu, 2019, 113 p.

122. **Kalev Erme**. The effect of catalysts in plasma oxidation of nitrogen oxides. Tartu, 2019, 114 p.

123. **Sergey Koshkarev.** A phenomenological feasibility study of the possible impact of the intrinsic heavy quark (charm) mechanism on the production of doubly heavy mesons and baryons. Tartu, 2020, 134 p.

124. **Kristi Uudeberg.** Optical Water Type Guided Approach to Estimate Water Quality in Inland and Coastal Waters. Tartu, 2020, 222 p.

125. **Daniel Blixt.** Hamiltonian analysis of covariant teleparallel theories of gravity. Tartu, 2021, 142 p.

126. **Ulbossyn Ualikhanova.** Gravity theories based on torsion: theoretical and observational constraints. Tartu, 2021, 154 p.

127. **Iaroslav Iakubivskyi**. Nanospacecraft for Technology Demonstration and Science Missions. Tartu, 2021, 177 p.

128. **Heido Trofimov.** Polluted clouds at air pollution hot spots help to better understand anthropogenic impacts on Earth's climate. Tartu, 2022, 96 p.

129. **Ott Rebane.** *In situ* non-contact sensing of microbiological contamination by fluorescence spectroscopy. Tartu, 2022, 157 p.